PCT WORLD INTELLECTUAL PROPERTY ORGANIZATION
International Bureau

INTERNATIONAL APPLICATION PUBLISHED UNDER THE PATENT COOPERATION TREATY (PCT)

(51) International Patent Classification 6 : A61K 38/10

A1

(11) International Publication Number: **WO 99/13899**

(43) International Publication Date: 25 March 1999 (25.03.99)

(21) International Application Number: PCT/US97/16850

(22) International Filing Date: 17 September 1997 (17.09.97)

(71) Applicants *(for all designated States except US)*: TRUSTEES OF THE UNIVERSITY OF PENNSYLVANIA [US/US]; Suite 300, 3700 Market Street, Philadelphia, PA 19104-3147 (US). THE BURNHAM INSTITUTE [US/US]; 10901 North Torrey Pines Road, La Jolla, CA 92037 (US).

(72) Inventors; and

(75) Inventors/Applicants *(for US only)*: LAMBRIS, John, D. [US/US]; 36 Haymarket Lane, Bryn Mawr, PA 19010 (US). MORIKIS, Dimitrios [GR/US]; 1355 Iverson Place, Riverside, CA 92506 (US).

(74) Agents: REED, Janet, E. et al.; Dann, Dorfman, Herrell and Skillman, Suite 720, 1601 Market Street, Philadelphia, PA 19103 (US).

(81) Designated States: AL, AM, AT, AU, AZ, BA, BB, BG, BR, BY, CA, CH, CN, CU, CZ, DE, DK, EE, ES, FI, GB, GE, HU, ID, IL, IS, JP, KE, KG, KP, KR, KZ, LC, LK, LR, LS, LT, LU, LV, MD, MG, MK, MN, MW, MX, NO, NZ, PL, PT, RO, RU, SD, SE, SG, SI, SK, TJ, TM, TR, TT, UA, UG, US, UZ, VN, YU, ZW, ARIPO patent (GH, KE, LS, MW, SD, SZ, UG, ZW), Eurasian patent (AM, AZ, BY, KG, KZ, MD, RU, TJ, TM), European patent (AT, BE, CH, DE, DK, ES, FI, FR, GB, GR, IE, IT, LU, MC, NL, PT, SE), OAPI patent (BF, BJ, CF, CG, CI, CM, GA, GN, ML, MR, NE, SN, TD, TG).

Published
With international search report.

(54) Title: PEPTIDES AND PEPTIDOMIMETICS FOR INHIBITING COMPLEMENT ACTIVATION

(57) Abstract

Peptides capable of inhibiting complement activation are provided. Methods of inhibiting complement activation and complement-mediated tissue injury using these peptides are also provided. In addition, a method of producing compositions capable of inhibiting complement activation using these peptides is provided, along with the peptide analogs and peptidomimetics produced by the method.

FOR THE PURPOSES OF INFORMATION ONLY

Codes used to identify States party to the PCT on the front pages of pamphlets publishing international applications under the PCT.

AL	Albania	ES	Spain	LS	Lesotho	SI	Slovenia
AM	Armenia	FI	Finland	LT	Lithuania	SK	Slovakia
AT	Austria	FR	France	LU	Luxembourg	SN	Senegal
AU	Australia	GA	Gabon	LV	Latvia	SZ	Swaziland
AZ	Azerbaijan	GB	United Kingdom	MC	Monaco	TD	Chad
BA	Bosnia and Herzegovina	GE	Georgia	MD	Republic of Moldova	TG	Togo
BB	Barbados	GH	Ghana	MG	Madagascar	TJ	Tajikistan
BE	Belgium	GN	Guinea	MK	The former Yugoslav Republic of Macedonia	TM	Turkmenistan
BF	Burkina Faso	GR	Greece			TR	Turkey
BG	Bulgaria	HU	Hungary	ML	Mali	TT	Trinidad and Tobago
BJ	Benin	IE	Ireland	MN	Mongolia	UA	Ukraine
BR	Brazil	IL	Israel	MR	Mauritania	UG	Uganda
BY	Belarus	IS	Iceland	MW	Malawi	US	United States of America
CA	Canada	IT	Italy	MX	Mexico	UZ	Uzbekistan
CF	Central African Republic	JP	Japan	NE	Niger	VN	Viet Nam
CG	Congo	KE	Kenya	NL	Netherlands	YU	Yugoslavia
CH	Switzerland	KG	Kyrgyzstan	NO	Norway	ZW	Zimbabwe
CI	Côte d'Ivoire	KP	Democratic People's Republic of Korea	NZ	New Zealand		
CM	Cameroon			PL	Poland		
CN	China	KR	Republic of Korea	PT	Portugal		
CU	Cuba	KZ	Kazakstan	RO	Romania		
CZ	Czech Republic	LC	Saint Lucia	RU	Russian Federation		
DE	Germany	LI	Liechtenstein	SD	Sudan		
DK	Denmark	LK	Sri Lanka	SE	Sweden		
EE	Estonia	LR	Liberia	SG	Singapore		

PEPTIDES AND PEPTIDOMIMETICS FOR INHIBITING COMPLEMENT ACTIVATION

Pursuant to 35 U.S.C. §202(c), it is acknowledged that the U.S. Government may have certain rights in the invention described herein, which was made in part with funds from the National Institutes of Health.

FIELD OF THE INVENTION

This invention relates to activation of the complement cascade in the body. In particular, this invention provides peptides and peptidomimetics capable of binding the C3 protein and inhibiting complement activation.

BACKGROUND OF THE INVENTION

Complement is a group of related plasma proteins that participate in inflammatory reactions. The activation of complement by classical, alternative and lectin pathways generates kinins from platelets, eosinophils and neutrophils. This activation is important in phagocytosis and curtailing infection.

Although complement is an important line of defense against pathogenic organisms, its activation can also lead to host cell damage. Complement-mediated tissue injury has been reported in a wide variety of diseases, including autoimmune diseases such as experimental allergic neuritis, type II collagen-induced arthritis, myasthenia gravis, hemolytic anemia, glomerulonephritis and immune complex-induced vasculitis. It has also been identified in the adult respiratory distress syndrome, stroke, heart attack, xenotransplantation, multiple sclerosis, burn injuries, extracorporeal dialysis and blood oxygenation.

The third complement component, C3, is known to have an important role in all of the pathways of

complement activation. Proteolytic activation of C3 by classical (C4b,2a) or alternative (C3b,Bb) pathway C3 convertase leads to cleavage of C3 into an anaphylotoxic peptide C3a and an opsonic fragment C3b. Covalent attachment of metastable C3b to target cells undergoing complement attack results in generation of C5a and formation of C5b-9 membrane attack complex. However, the tissue injury that results from complement activation is directly mediated by the membrane attack complex, C5b-C9, and indirectly by the generation of anaphylotoxic peptides C3a and C5a. These peptides induce damage through their effect on neutrophils and mast cells. Upon stimulation with C5a, neutrophils produce a serine elastase that causes tissue injury. C5a also triggers the generation of toxic oxygen-derived free radicals from neutrophils, and both C3a and C5a stimulate rapid and enhanced production of leukotrienes from IL-3-primed basophils.

Control of the activation process is mediated *in vivo* by a family of structurally and functionally related proteins termed regulators of complement activation (hereinafter referred to as RCA). The RCA include both plasma proteins, i.e. factor H and C4 binding protein (C4bp) and membrane proteins, i.e., complement receptor 1 (CR1), decay-accelerating factor (DAF) and membrane cofactor protein (MCP). These proteins inhibit the generation of C3a and C5a by inactivating the C3 and C5 convertases of the classical and alternative pathways. Inhibition of complement activation by these proteins is achieved by dissociation of the subunits of C3 and C5 convertases and/or by proteolytic inactivation of the subunits by factor I.

The importance of complement-mediated tissue injury via a wide variety of disease states underscores the growing need for a specific complement inhibitor. Various approaches have been used to identify such an inhibitor. These include targeting the serine proteases

with peptides or chemical compounds. PCT/US95/02945 disclose chimeric complement inhibitor proteins having a first functional domain with C3 inhibitory activity and a second functional domain with C5b-9 inhibitory activity. More recently attempts have been made to target the thioester of C3. For example, salicyl hydroxamate, believed to be one of the most potent inhibitors of C3, inhibits complement by reacting with the thioester of C3 (Sim et al. *Biochem. J.* 1981 **193**:115). The 50% inhibitory concentrations required for the inhibition of classical and alternative pathway-mediated hemolytic activities with this compound were 280 μM and 33 μM, respectively. However, salicyl hydroxamate has been reported to produce systemic lupus erythematosus-like syndrome as a toxic side effect (Sim et al. *Lancet* 1984 ii:422). Kalli et al. demonstrated that a soluble form of CR1 (sCR1) suppresses complement in several complement-dependent disease models (*Springer Semin. Immunopathol.* 1994 **15**:417).

In view of the foregoing discussion, a need clearly exists for small molecule inhibitors of complement activation. It is an object of the present invention to provide peptides and peptide analogs or mimetics that perform this function.

SUMMARY OF THE INVENTION

According to one aspect of the present invention, peptides and peptide analogs and mimetics that inhibit complement activation are provided. These peptides and mimetics are referred to collectively herein as "complement-inhibiting compounds." According to one aspect of the invention, exemplary peptides are provided that comprise at least a portion of the amino acid sequence of the N-terminal cyclic region of a peptide of Sequence I.D. No. 1. In a preferred embodiment, the peptides of the present invention comprise at least the 13 amino acid sequence of Sequence I.D. No. 2.

According to another aspect of the invention, a method is provided for inhibiting complement activation in a patient. The method comprises administering to a human an effective amount of a complement-inhibiting compound of the present invention.

According to another aspect of the invention, a method is provided for treating complement-mediated tissue injury in a patient. The method comprises administering to a patient an effective amount of a complement-inhibiting compound of the present invention.

According to another aspect of the invention, a method is provided for inhibiting complement activation which occurs during use of artificial organs or implants. The method comprises coating the artificial organ or implant with a complement-inhibiting compound of the present invention.

According to another aspect of the invention, a method is provided for inhibiting complement activation that occurs during extracorporeal shunting of physiological fluids (e.g. blood, urine). The method comprises coating the tubing through which said fluids are shunted with a peptide of the present invention.

According to another aspect of the invention, a method is provided for producing compounds, such as peptide analogs or peptidomimetics, capable of inhibiting complement activation. The method comprises identifying the conformation of a peptide having Sequence I.D. No. 1 or Sequence I.D. No.2, which is capable of interacting with C3 to inhibit complement activation, and producing a compound having a sufficiently similar conformation so that the compound interacts with C3 to inhibit complement activation.

Yet another aspect of the invention provides a compound having sufficiently similar conformation to the peptide having Sequence I.D. No.1 or Sequence I.D. No.2 such that the compound is capable of interacting with C3 to inhibit complement activation. Examples of such

compounds include peptide analogs of Sequence I.D. No.1 or Sequence I.D. No.2, having conservative amino acid substitutions, i.e. substitutions that do not materially alter the structure of the analog as compared to SEQ ID NOS: 1 or 2, and having complement-inhibiting activity. Other examples include peptidomimetics having sufficiently similar conformation to SEQ ID NOS: 1 or 2 so as to exhibit complement-inhibiting activity.

According to another aspect of the invention, a compound comprising an analog of a disulfide bridged form of Sequence I.D. No. 2 is provided, which includes a segment corresponding to the tetrapeptide segment of Sequence I.D. No. 2 that includes residues 5 through 8, the segment having a constrained backbone conformation comprising a Type I β-turn. The compound is capable of binding to C3 and inhibiting complement activation. In preferred embodiments, the aforementioned compound comprises the central portion of a larger analog that also includes: (1) an N-terminal portion of flexible structure that preferably is an analog of residues 2 through 4 (more preferably 1 through 4) of Sequence I.D. No. 2, and preferably wherein the analog of residue 3 comprises a hydrophobic side chain and the analog of residue 2 is capable of forming a covalent bond with another atom of length and angle equivalent to a disulfide bond; and (2) a C-terminal portion of flexible structure that preferably is an analog of residues 9 through 12 (more preferably 9 through 13) of Sequence I.D. No. 2, preferably wherein the analog of residue 12 is capable of forming a covalent bond with the analog of residue 2, of length and angle equivalent to a disulfide bond.

BRIEF DESCRIPTION OF THE DRAWINGS

Figure 1 is a bargraph showing specific binding of a C3 binding clone isolated from a phage-displayed random peptide library to C3 and C3 fragments including:

C3b, the proteolytically activated form of C3; C3c, 135,300 Mr fragment of C3 generated using elastase; and C3d, 35,000 Mr fragment of C3 generated using elastase. Microtiter wells were coated with 2 μg of C3, C3b, C3c or C3d, saturated with blocking buffer, washed with PBS (pH 7.4) containing 0.05% Tween 20, and incubated 1 hour at 22°C with a positive (clone 9) or negative (clone 1) clone. Binding was inhibited by adding 250 μg/ml of aggregated C3 in PBS, pH 7.4. Bound M13 phage particles were detected by peroxidase-coupled anti-M13 antibody and ABTS peroxidase substrate. Diagonally lined bars represent peroxidase-coupled anti-M13 antibody bound non-specifically to the plate; cross-hatched bars represent clone 9 bound to C3 or C3 fragments; horizontally lined bars represent clone 9 bound to C3 or C3 fragments in the presence of 250 μg/ml of aggregated C3; and vertically lined bars represent clone 1 bound to C3 or C3 fragments.

Figure 2 is a linegraph showing the binding of peptide I to C3 and C3 fragments. A microtiter plate was coated with peptide I, saturated with blocking buffer, washed with PBS (pH 7.4) containing 0.05% Tween 20, and incubated with two-fold dilutions of C3 (●), C3b (■), C3c (▲) or C3d (▼) for 1 hour at 22°C. The plate was then washed and incubated with a polyclonal rabbit anti-C3 antibody (2 μg/ml) and a 1:1000 dilution of peroxidase-coupled anti-rabbit antibody. Color was developed with the ABTS peroxidase substrate.

Figure 3 is a linegraph showing inhibition of classical and alternative pathway-mediated lysis of erythrocytes by peptides of the present invention. Cyclic peptides (peptide I (●) and peptide IV (Compstatin) (▲)) and reduced and alkylated peptides (peptide II (■) and V (▼)) were tested for their effect on the alternative (panel A) and classical (panel B) pathways of complement activation.

Figure 4 shows inhibition of C3 cleavage by peptide IV (Compstatin) during alternative pathway

activation in normal human serum (hereinafter referred to as NHS). Cleavage of C3 was measured by incubating NHS containing ^{125}I-C3 (0.5 μCi) with 5 mM MgEGTA, zymosan, and increasing concentrations of peptide IV for 30 minutes at 37°C. Samples were run on 7.5% SDS-PAGE under reducing conditions and the gel was subjected to autoradiography. Radioactive bands were cut out and counted. The data were normalized by considering 100% cleavage of C3 to be equal to the amount of C3 cleaved in the absence of peptide IV. Controls contained 10 mM EDTA. The reduced and alkylated peptide V (200 μM) was included as a control peptide.

Figure 5 shows inhibition of C3 cleavage by peptide IV (Compstatin) during activation of the alternative pathway reconstituted with purified components. The alternative pathway was reconstituted by adding C3 and factors B and D, and various concentrations of the peptide IV were added. Samples were analyzed by running on 7.5% SDS-PAGE under reducing conditions. The gel was stained with Coomassie Blue and the intensity of each band was determined by densitometric analysis. Data were normalized by considering 100% cleavage of C3 to be equal to the cleavage observed in the absence of peptide IV. Controls contained EDTA. The reduced and alkylated peptide V (200 μM) was included as a control peptide.

Figure 6 shows the effect of peptide IV (Compstatin) on factor B cleavage. Factor B cleavage was quantitated by incubating C3b with factor B, factor D and various concentrations of peptide IV (6 μM - 400 μM) in the presence of MgEGTA for 1 hour at 37°C. Samples were analyzed on 7.5% SDS-PAGE in the presence of DTT. The gel was stained and scanned for densitometric analysis. The reduced and alkylated peptide V (200 μM) was included as a control peptide. Controls were set by adding 10 mM EDTA.

Figure 7 is a bargraph showing the effect of peptide IV (Compstatin) on properdin binding to C3 coated

to a microtiter plate. C3 (20 μg/ml) was coated onto microtiter wells and incubated with NHS containing 10 mM EDTA and graded concentrations of peptide IV for 1 hour at 22°C. Binding of properdin was detected by a polyclonal goat anti-properdin antibody (10 μg/ml) and a 1:1000 dilution of peroxidase-conjugated anti-goat antibody. The reduced and alkylated peptide V was included as a control peptide.

Figure 8 shows a portion of the 500 MHz 2D TOCSY spectrum of Compstatin. All thirteen spin systems are identified, and individual spins within the same spin system are connected with lines. The right panel shows the spin system of Ile^1 originating from the α-proton, since the NH of the first residue in the sequence is not observable due to fast exchange with the solvent. The arrows point to NH-H^α cross peaks of Cys^2 and Cys^{12} outside the limits of the plot. These cross peaks are very weak because their H^α-resonances are close to the solvent water resonance and they are attenuated by the water presaturation scheme of the data acquisition pulse sequence. However, the NH-H^α cross peak of Cys^{12} is observed at a lower contour level, and the NH-H^α cross peak is present in the DQ, DQF-COSY and J-R NOESY spectra. Some TOCSY connectivities involving the Arg^{11} $Nh^{\varepsilon 15}$ and long range couplings between aromatic and side chain protons are also shown. Sample conditions are pH 6 and 5°C.

Figure 9 shows scalar $^3J_{NH\text{-}H\alpha}$-coupling constants extracted from a DQF-COSY spectrum. Circles correspond to coupling constants evaluated using the Kim and Prestegard (J. Mag. Res. 84: 9-13, 1989) procedure, squares correspond to the raw peak-to-peak separation of the antiphase components of the DQF-COSY cross peaks, triangles and inverted triangles correspond to an automatic fitting procedure and an averaged manual measurement, respectively, of the coupling constants provided by the program Felix 2.3 (Biosym Technologies,

San Diego). Details of the evaluation of $^3J_{NH-H\alpha}$-coupling constants are given in Example 5. $^3J_{NH-H\alpha}$-coupling constants with values higher or lower than the straight dotted line correspond to two or four, respectively, real solutions of the Karplus equations. The Karplus equations are evaluated with coefficients A=6.98, B=-1.38, C=1.72 (Wang and Bax, 1996). Data were obtained at pH 6 and 5° C.

Figure 10 shows the solution structure of Compstatin in three different formats. The structure on the left shows the backbone and the disulfide bond of the ensemble of the family of the final refined 21 structures of Compstatin. The average RMSD for the backbone heavy atoms was 0.6 Å and for all heavy atoms was 1.2 Å. The structure in the center shows the Type I β-turn segment of the averaged restrained regularized structure of Compstatin spanning the residues Gln^5-Asp^6-Trp^7-Gly^8. The structure on the right shows a space-filling model of Compstatin.

Figure 11 shows the results of structural analyses of Compstatin. The upper panel shows the number of intra-residue (solid black), backbone-backbone and H^β-backbone (grey) and other medium and long-range (white) NOE constraints per residue used in the structure calculations of Compstatin. The center panel shows the backbone heavy atom RMSD (squares) and all heavy atom RMSD (circles) per residue for the ensemble of the family of the final refined 21 structures of Compstatin. The lower panel shows the calculated fractional solvent accessibility per residue of Compstatin.

Figure 12 shows results of chemical shift measurements of Compstatin. The upper panel shows the difference between the measured chemical shift of the H^α-protons of Compstatin and the chemical shift values of H^α-protons of amino acids in random coil peptides (Merutka et al., J. Biom. NMR 5: 14-24, 1995) for each residue of Compstatin. Data were obtained at pH 6 and 5°C. The

lower panel shows the difference between the measured chemical shifts of NH protons of Compstatin at 10°C and 5°C. Chemical shift differences between the solid lines correspond to temperature coefficients of NH-protons of amino acids in random coil peptides. Chemical shift differences higher than the dotted line correspond to temperature coefficients of NH-protons that could be hydrogen-bonded.

DETAILED DESCRIPTION OF INVENTION

Peptides that inhibit complement activation have now been identified. The peptides of the present invention comprise at least a portion of the N-terminal cyclic region of a peptide of Sequence I.D. No.1. In a preferred embodiment, the peptides of the present invention comprise at least the 13 amino acid sequence of Sequence I.D. No.2. Analogs and mimetics of Sequence I.D. No.1 and Sequence I.D. No.2 are also within the scope of this invention.

To initially identify C3-binding, complement-inhibiting peptides of the invention, a phage-displayed random peptide library was screened for binding to C3b, the proteolytically activated form of complement component C3. A phage-displayed peptide was identified, which bound to C3, C3b and C3c, but not to C3d, indicating that it binds to the C3c region of C3. A synthetic 27-amino acid peptide corresponding to the phage-displayed peptide (Peptide I, Sequence I.D. No. 1) also bound to C3 and C3 fragments and inhibited both the classical and alternative pathways of complement activation. The inhibition of complement activation was reversible.

Analysis of overlapping peptides indicates that the functional activity of Peptide I is located in the cyclic 13-amino acid N-terminal region, referred to herein as "Compstatin" or "Peptide IV". Compstatin

comprises the following sequence (Sequence I.D. No. 2), with a disulfide bridge between Cys^2 and Cys^{12}:

Ile^1-Cys^2-Val^3-Val^4-Gln^5-Asp^6-Trp^7-Gly^8-His^9-His^{10}-Arg^{11}-Cys^{12}-Thr^{13}

Destruction of the disulfide bridge by reduction and alkylation of Compstatin destroys its inhibitory activity. Compstatin inhibits C3 cleavage in normal human serum as well as when the alternative pathway is reconstituted with purified complement components. The inhibition appears not to be due to sterically hindered access to the C3a/C3b cleavage site. Further, the peptide does not inhibit the cleavage of Factor B, indicating that it does not affect the interaction of C3b with factor B or the formation of C3b,Bb. The peptide also has no effect on the binding of properdin to C3, demonstrating that the inhibition of C3 cleavage in normal human serum is not due in part to its effect on the properdin-stabilized C3 convertase, C3b,Bb,P.

The proteolytically activated form of C3, C3b, binds to more than 20 serum and membrane proteins, most of which belong to a superfamily of structurally and functionally related molecules. However, in native C3 the binding sites for these proteins are buried and become available only after the conformational change that occurs upon the cleavage of C3 to C3b. The data presented hereinbelow (Example 1, Figures 1, 2, and 5) makes it clear that Compstatin (and Peptide I) bind to native C3 and inhibit its activation. Thus, the inhibition of complement with these inhibitory peptides not only inhibits the generation of C5a but also of C3a.

Synthetic peptides of the present invention which are analogous to the identified phage-displayed C3-binding peptide were able to inhibit the alternative pathway of complement activation at a concentration that was only two-fold greater than the concentration of C3 in NHS (Figure 3 and Table 1). The concentration required

to inhibit the classical pathway was 5-fold higher than that required to inhibit the alternative pathway thus indicating that the inhibitory action of the peptides of the present invention is probably directed toward the activation of C3 or C3 convertase. Accordingly, the peptides of the present invention are believed to be useful as therapeutics in diseases involving complement-mediated damage. Examples of complement-mediated diseases include, but are not limited to, autoimmune diseases such as experimental allergic neuritis, type II collagen-induced arthritis, myasthenia gravis, hemolytic anemia, glomerulonephritis, and immune complex-induced vasculitis, adult respiratory distress syndrome, stroke, heart attack, xenotransplantation, multiple sclerosis, burn injuries, extracorporeal dialysis and blood oxygenation. Thus, in the present invention, patients suffering from a disease involving complement-mediated damage can be administered an effective amount of a peptide of the invention so that complement activation is inhibited. By "effective amount" it is meant a concentration of peptide which is capable of inhibiting complement activation. Such concentrations can be routinely determined based upon *in vitro* data such as that provided herein. Appropriate modes of administration, dose ranges and pharmaceutical vehicles can also be routinely determined by those of skill in the art in accordance with the disease to be treated and the patient profile.

The compositions of the present invention will also find use in other situations in which inhibition of complement activation is desired. For instance, complement activation that occurs in xenographic or allographic transplant may be inhibited by administering a peptide of the invention to a patient receiving such transplant, or by coating organs with a peptide of the invention. Further, the peptides of the present invention can be used to coat biomaterials used in

artificial organs and implants to inhibit complement activation which occurs during use of these artificial materials.

To demonstrate the efficacy of the peptides of the invention to inhibit complement activation in xenographic transplantation, we have tested the effect of Compstatin in a xenotransplantation model (Fiane et al., Transpl. Proc. 27: 3560-3561, 1995). Porcine kidneys were perfused with human blood containing Compstatin (48-60 mg/450 ml blood) and time of rejection was monitored. Rejection was defined as 100% increase of resistance in renal flow and marked macroscopic changes with patchy hemorrhage and swelling of the perfused kidney. Controls were perfused with human blood containing reduced and alkylated Compstatin. It was found that addition of the Compstatin to the human blood resulted in a survival of the kidney for 6-7 hours (which corresponds to the limit of the model), as compared to survival of 1.5-2 hours in the control kidney.

As another example, complement activation during extracorporeal shunting of physiologic fluid may be inhibited by coating tubing through which the fluids flow with a peptide of the invention. This method can be applied to a variety of extracorporeal shunting techniques, including hemodialysis, kidney dialysis and cardiopulmonary bypass circuits. To demonstrate this use of the peptides of the invention, the following experiment was performed. Five ml of freshly drawn blood containing 0.8 IU heparin/ml was rotated for 1 hr at 37°C and thereafter analyzed for blood cell counts, hemolysis, C3a concentration, terminal complement complex (TCC) concentration and expression of CR3 (CD11b) on polymorphonuclear leukocytes (PMNLs). Compstatin corresponding to 4-, 8-, and 12-fold (60 μM) molar excess (compared to C3 concentration in blood) was used. Blood cell counts, including platelets (approx. 230 x 10^9/L) remained stable during the incubation, and no hemolysis

was noted, suggesting that the peptide was not toxic to the cells. Generation of C3a and TCC and expression of CR3 on PMNLs were all significantly reduced, even at only a 4-fold molar excess of Compstatin. At 60-fold excess of Compstatin to C3, we were able to inhibit all previously-described functions.

The inhibitory activity of Compstatin and its analogs is highly specific to human C3. Compstatin and Peptide I had no inhibitory activity on the complement mediated lysis of rabbit erythrocytes by mouse or rat complement. Further, studies with these peptides in C3-knockout mice wherein hemolytic activity is reconstituted with human C3 showed inhibition at concentrations similar to those seen for human serum. Accordingly, initial testing of *in vivo* effectiveness of these peptides in various disease models would need to be performed in models such as transgenic mice expressing human C3 or alternatively, C3 knockout mice infused with human C3. The inhibitory activity of Compstatin on guinea pig, swine and monkey complement was also determined. The peptide inhibited monkey complement but failed to inhibit guinea pig or swine complement. Complement inhibition in Rhesus monkeys, cynomolgus monkeys and baboons was comparable to that in humans.

The rate of clearance of a protein or peptide is an important determinant of its biological effects. Accordingly, the *in vivo* half-life of a peptide of the present invention was determined in SJL mice. A peptide of the invention containing tyrosine residues at its C-terminus (ICVVQDWGHHRCTAGHYY (Sequence I.D. No.23)), which demonstrated equal activity to Compstatin in a hemolytic assay, was used. This peptide showed a heterogeneous clearance rate, with a $t_{1/2}$ of 11 hours.

Due to the specificity for C3 and effectiveness of the peptides of the present invention, they can also be used as reagents to inhibit C3 activation in *in vitro* assay systems. In addition, the specificity of these

peptides to C3 makes them very useful in further elucidating the importance of different components in the complement cascade.

Peptides of the present invention, especially Sequence I.D. No.1 and Sequence I.D. No.2, are also useful to identify specific conformational features required for the peptide to interact with C3 and inhibit complement activation. Examples of a structure-function analyses using various analogs is described in Examples 1, 2 and 3. Example 1 describes a series of substitution and size reduction analogs of Compstatin; Example 3 provides additional examples of such analogs. Example 2 describes analysis of a retro-inverso peptidomimetic of a peptide of the invention to reveal the relative importance of main chain versus side-chain amino acid configurations in the complement-inhibitory activity of the peptide.

Thus, several exemplary Compstatin analogs have been, or can be, synthesized, which can bind to C3 and inhibit complement activation. These peptides can be described generally by the formula:

X1-X2-X3-X4-X5-X6-X7-X8-X9-X10-X11-X12-X13,

wherein:

X1 is absent or is any amino acid (preferably Ile);

X2 is Cys, or a residue with an acidic side chain, such as Glu or Asp (provided the residue at X12 contains a basic side chain (such as Lys or Arg), or a residue with a basic side chain (such as Lys or Arg), provided that the residue at X12 contains an acidic side chain (such as Glu or Asp);

X3 is Val, Leu, Phe, Ile, Met or Trp;

X4 is Val, Leu, Phe, Ile, Met or Trp;

X5 is Gln, Asn, Asp, Ser or Ala;

X6 is Asp, Glu, Ser, Thr or Pro;

X7 is Trp, Phe, Ile, Val, Leu, Met, His, Tyr, Asp, Ser, Asn, Arg or Gly;

X8 is Gly;

X9 is any amino acid, preferably His or Ala;

X10 is any amino acid, preferably His or Ala;

X11 is any amino acid, preferably Arg or Ala;

X12 is Cys, or a residue with an acidic side chain, such as Glu or Asp (provided the residue at X2 contains a basic side chain (such as Lys or Arg), or a residue with a basic side chain (such as Lys or Arg), provided that the residue at X2 contains an acidic side chain (such as Glu or Asp); and

X13 is absent or is any amino acid, preferably Thr.

The residues listed above can also be modified, e.g., as described in greater detail in Example 3.

Other approaches to determine the structures of peptides of the invention have also been used. In accordance with the present invention, we have now determined the solution structure of Compstatin using a two-dimensional NMR technique. We have generated an ensemble of a family of solution structures of the peptide with a hybrid distance geometry-restrained simulated annealing methodology, using distance, dihedral angle and $^{3}J_{NH-H\alpha}$-coupling constant restraints. The Compstatin structure has been determined to contain a

Type I β-turn comprising the segment Gln^5-Asp^6-Trp^7-Gly^8. Preference for packing of the hydrophobic side chains of Val^3, Val^4 and Trp^7 is observed. The generated structure has been analyzed for consistency using NMR parameters such as NOE connectivity patterns, $^3J_{NH\text{-}H\alpha}$-coupling constants and chemical shifts. As discussed above, analysis of Ala substitution analogs suggested that Val^3, Gln^5, Asp^6, Trp^7 and Gly^8 contribute significantly to the inhibitory activity of the peptide. Substitution of Gly^8 caused a 100-fold decrease in inhibitory potency. In contrast, substitution of Val^4, His^9, His^{10} and Arg^{11} resulted in minimal change in the activity. Taken together, these findings indicate that the β-turn is critical for preservation of the functional activity of Compstatin and that residues Gln^5-Gly^8 form the binding site for C3. The structural features of Compstatin are described in greater detail in Example 5.

Using the aforementioned approaches, compositions having sufficiently similar conformations can be produced and tested for their ability to inhibit complement activation. By "sufficiently similar" it is meant a conformation which is capable of interacting with C3 and inhibiting complement activation. Further, C3 knockout mice or mice expressing human C3 can be used in studying structure/function relationships of human C3, either by blocking specific function with anti-C3 monoclonal antibodies or by infusing mutant forms of C3.

Once a particular desired conformation of a short peptide has been ascertained, methods for designing a peptide or peptidomimetic to fit that conformation are well known in the art. See, e.g., G.R. Marshall (1993), Tetrahedron, 49: 3547-3558; Hruby and Nikiforovich (1991), in Molecular Conformation and Biological Interactions, P. Balaram & S. Ramasehan, eds., Indian Acad. of Sci., Bangalore, PP. 429-455). The design of peptide analogs may be further refined by considering the contribution of various side chains of amino acid

residues, as discussed above (i.e., for the effect of functional groups or for steric considerations).

It will be appreciated by those of skill in the art that a peptide mimic may serve equally well as a peptide for the purpose of providing the specific backbone conformation and side chain functionalities required for binding to C3 and inhibiting complement activation. Accordingly, it is contemplated as being within the scope of the present invention to produce C3-binding, complement-inhibiting compounds through the use of either naturally-occurring amino acids, amino acid derivatives, analogs or non-amino acid molecules capable of being joined to form the appropriate backbone conformation. A non-peptide analog, or an analog comprising peptide and non-peptide components, is sometimes referred to herein as a "peptidomimetic" or "isosteric mimetic," to designate substitutions or derivations of the peptides of the invention, which possess the same backbone conformational features and/or other functionalities, so as to be sufficiently similar to the exemplified peptides to inhibit complement activation.

The use of peptidomimetics for the development of high-affinity peptide analogs is well known in the art (see, e.g., Zhao et al. (1995), Nature Structural Biology 2: 1131-1137; Beely, N. (1994), Trends in Biotechnology 12: 213-216; Hruby, V.J. (1993), Biopolymers 33: 1073-1082). Assuming rotational constraints similar to those of amino acid residues within a peptide, analogs comprising non-amino acid moieties may be analyzed, and their conformational motifs verified, by means of the Ramachandran plot (see Hruby & Nikiforovich, *supra*), among other known techniques.

In accordance with the present invention, an analog of Compstatin comprises the basic backbone conformation as follows: (1) an N-terminal portion (preferably including at least 3 amino acid residues or

isosteric mimetics) having a flexible conformation; (2) a central portion (preferably of at least 3 amino acid residues or mimetics) comprising a β-turn (preferably Type I); and a C-terminal portion (preferably including at least 4 amino acid residues or mimetics) having a flexible conformation. In correspondence with Compstatin, for example, the aforementioned N-terminal portion corresponds to residues 1 or 2 through 4; the central portion corresponds to residues 5 through 8; and the C-terminal portion corresponds to residues 9 through 12 or 13. Of these three features, the analog should, at minimum, possess a conformationally stabilized β-turn (preferably Type I) in the central portion. In preferred embodiments, the turn is stabilized by virtue of a disulfide bond (or equivalent thereof) between residues or mimetics corresponding to residues 2 and 12 of Compstatin. In other preferred embodiments, the N-terminal segment comprises a residue or mimetic having a hydrophobic side chain at a position corresponding to residue 3 and, optionally, residue 4 of Compstatin; and the central portion comprises a residue or mimetic having a hydrophobic side chain at a position corresponding to residue 7 of Compstatin.

The following nonlimiting examples are provided to further illustrate the present invention.

EXAMPLE 1
Inhibition of Human Complement by a C3-Binding Peptide Isolated from a Phage-Displayed Random Peptide Library

MATERIALS AND METHODS

Chemicals and buffers. All chemicals and reagents used for peptide synthesis were purchased from Applied Biosystems (Foster City, CA), with the exception of Fmoc amino acids, which were obtained from Nova Biochem (San Diego, CA). Veronal-buffered saline (VBS), pH 7.4, contained 5 mM barbital and 145 mM NaCl. Gelatin veronal-buffered saline (GVB) was VBS containing 0.1%

gelatin, GVB^{++} was GVB containing 0.5 mM $MgCl_2$ and 0.15 mM $CaCl_2$, and GVBE was GVB with 10 mM EDTA. MgEGTA, contained 0.1 M $MgCl_2$ and 0.1 M EGTA. Phosphate-buffered saline (PBS), pH 7.4, contained 10 mM phosphate and 145 mM NaCl. Blocking buffer was PBS containing 0.5% milk and 1% bovine serum albumin (BSA).

Purified complement components. Human complement proteins C3, factor B, factor H and factor I were purified from normal human plasma in accordance with well known procedures. The C3 used in these experiments was a mixture of 72% native C3 and 28% C3(H_2O), as determined by analyzing a sample of the protein on a Mono S column (Pharmacia, Piscataway, NJ) in accordance with procedures described by Pangburn, M.K. (J. Immunol. Methods 102: 7, 1987). C3b was generated by limited trypsin cleavage of C3 and purified on a Mono Q column (Pharmacia) in accordance with procedures described by Becherer and Lambris (Journal of Biological Chemistry 263: 14586, 1988). C3c and C3d were generated by elastase treatment of C3 and purified on a Mono Q column as also described by Becherer and Lambris. Aggregated C3 was made using glutaraldehyde in accordance with procedures described by Erdei et al. (Eur. J. Immunol. 1985 15: 184, 1985). For iodination, native C3 was separated from C3(H_2O) on a Mono S column and radiolabeled using ^{125}I and Iodogen (Pierce Chemical Co., Rockford, IL). The specific activity of the labeled C3 varied from 1.0 to 2.5 $\mu Ci/\mu g$.

Construction of the phage library. The library consisted of 2 x 10^8 recombinants, each expressing the peptide sequence SR X_{12} (S, P, T, or A) A (V, A, D, E, or G) X_{12} SR, at the N-terminus of pIII. Fixed and semi-fixed amino acids (due to oligonucleotide design) are underlined. The library was constructed in accordance with procedures published by Kay et al. (Gene 128: 59, 1993). The random amino acids were encoded by NNK, where

N represents equimolar ratios of A, C, G, or T and K represents G or T. The NNK coding scheme utilizes 32 codons to encode 20 amino acids; the frequency of each amino acids is once (C, D, E, F, H, I, K, M, N, Q, W, Y), twice (A, G, P, V, T), or thrice (L, R, S) per codon.

Biopanning of the phage library. The C3-binding phage was isolated by screening the phage library described above. Microtiter well plates (Nunc Inc., Naperville, IL) were coated overnight with 20 μg of C3b in PBS at 4°C and blocked with PBS containing 1% BSA for 30 minutes at 22°C. After washing, 6 x 10^{11} plaque-forming units of the library were added to each well and incubated overnight at 4°C. The wells were washed five times with PBS containing 0.1% Tween 20 and 0.1% BSA. Bound phage particles were eluted with 100 mM glycine-HCl, pH 2.3, and immediately neutralized with 100 mM Tris-HCl, pH 8.5. Recovered phage particles were amplified in DH5αF' *E. coli*. This biopanning procedure was repeated twice. The amplified phage mixture obtained after the third round of amplification was plated, and positive phage were identified by confirming their binding to C3b in an ELISA, in which bound phage were detected by peroxidase-labeled anti-M13 antibody (Pharmacia). DNA was prepared from positive phage stocks and subjected to dideoxy sequencing in accordance with well known procedures.

Synthesis and purification of peptides. Peptides were synthesized in an Applied Biosystem peptide synthesizer (model 431A) using Fmoc amide resin. The side chain protecting groups were: Cys(Trt), Asp(otBu), Arg (Pmc), Thr (tBu), Ser (tBu), Gln (Trt), Trp(Boc), His(Trt), Asn(Trt). Peptides were cleaved from the resin by incubation for 3 hours at 22°C with a solvent mixture containing 5% phenol, 5% thioanisole, 5% water, 2.5% ethanedithiol, and 82.5% trifluoroacetic acid (TFA). The

reaction mixture was filtered through a fritted funnel, precipitated with cold ether, dissolved in 50% acetonitrile containing 0.1% TFA, and lyophilized. The crude peptides obtained after cleavage were dissolved in 10% acetonitrile containing 0.1% TFA and purified using a reverse phase C-18 column (Waters, Milford, MA). Disulfide oxidation of purified peptides (SEQ ID NOs: 1, 2, 5-21) was performed by stirring a 0.15 mM solution of peptide in 0.1 M ammonium bicarbonate, pH 8.0, bubbling with oxygen at 22°C for 48 hours. Purified peptides I were reduced with 10 mM dithiothreitol (DTT) and alkylated with 40 mM iodoacetamide. The identity and purity of all peptides were confirmed by laser desorption mass spectroscopy.

Peptide binding to C3 and C3 fragments. Binding of synthetic peptide to C3 and to various fragments of C3 was evaluated by means of an ELISA. Microtiter plates (Nunc) were coated for 1 hour at 37°C with 100 µl of peptide I (Sequence I.D. No.1) at 400 µg/ml or with 10 µg/ml of peptide I (Sequence I.D. No.2) coupled to BSA (1:1, w/w), then saturated with blocking buffer for 30 minutes at 22°C. The plates were washed three times with PBS containing 0.05% Tween 20, and various amounts of C3 or C3 fragments were added. After incubation for 1 hour at 22°C, the wells were washed and incubated at 22°C for 1 hour with 100 µl of 2 µg/ml polyclonal rabbit anti-C3 antibody. Unbound anti-C3 antibodies were removed by washing, and a 1:1000 dilution of peroxidase-conjugated goat anti-rabbit IgG was added and incubated for 1 hour at 22°C. Color was developed by adding ABTS peroxidase substrate, and the optical density was read at 405 nm. Net binding was calculated by subtracting the readings obtained for nonspecific binding of C3 and C3 fragments to the plate in the absence of peptide.

Complement inhibition assays. Inhibition of classical and alternative pathway activity by the peptides was measured. To determine the effect of peptides on the classical pathway, various concentrations of peptide were mixed with 11 μl of normal human serum (NHS, diluted 1:10 in GVB^{++}) and 5 μl of sheep erythrocytes coated with antibodies (EA) (1 x 10^9/ml) and GVB^{++} was added to give a total volume of 250 μl. The reaction mixture was incubated at 37°C for 1 hour and centrifuged. The percentage of lysis was determined by measuring the optical density of the supernatant at 414 nm. The effect of peptides on the alternative pathway was determined by measuring the lysis of rabbit erythrocytes (Er) in normal human serum (NHS) as previously described (Sahu and Pangburn, 1996). Various concentrations of peptide were mixed with 5 μl of NHS, 5 μl of 0.1M MgEGTA and 10 μl of Er (1 x 10^9/ml) and brought to a final volume of 100 μl in GVB (5mM barbital, 0.1% gelatin and 145mM NaCl, pH 7.4). The reaction mixture was incubated at 37°C for 20 min and stopped by adding 200 μl of GVBE (GVB with 10mM EDTA). After centrifugation, lysis of Er was determined at 414 nm. The percentage of lysis obtained was normalized by considering 100% lysis to be equal to the lysis occurring in the absence of the peptide. The concentration of the peptide causing 50% inhibition of hemolytic activity was taken as the IC_{50}.

Measurement of C3 convertase-mediated cleavage of C3. Inhibition of C3 cleavage by peptide IV (Sequence I.D. No.2) in NHS was determined. Seven microliters of 35% NHS containing 0.5 μCi of ^{125}I-C3 and 14.3 mM MgEGTA were mixed with graded concentrations of peptide IV (Sequence I.D. No.2) and 4 μl of 50% zymosan. The total volume of the reaction mixture was adjusted to 20 μl by adding GVB. Samples were incubated at 37°C for 30 minutes, mixed with 10 μl of 30 mM EDTA, and centrifuged. The supernatant obtained was mixed with SDS sample buffer

containing 10 mM DTT, analyzed on a 7.5% SDS-PAGE gel, and subjected to autoradiography. Radioactive bands were excised and counted to calculate the percentage of C3 cleaved. The percentage of ^{125}I-C3 cleaved was normalized by considering 100% ^{125}I-C3 cleaved to be equal to the ^{125}I-C3 cleaved in the absence of the peptide. Controls were incubated in the presence of 10 mM EDTA.

The effect of peptide IV (Sequence I.D. No.2) on C3 cleavage by purified complement components was also determined. Two μg of C3 were incubated with various concentrations of the peptide at 37°C for 15 minutes. Thereafter, 2 μg of factor B and 0.04 μg of factor D were added in the presence of 5 mM MgEGTA, in a total volume of 20 μl, to activate the pathway. After 2 hours at 37°C, samples were run on a 7.5% SDS-PAGE gel, stained, scanned for densitometric analysis, and the percentage of C3 cleaved was calculated. The data obtained were normalized by considering 100% C3 cleavage to be equal to the amount of C3 cleaved in the absence of the peptide. Controls were incubated in the presence of 10 mM EDTA.

Measurement of factor B cleavage. The effect of peptide IV (Sequence I.D. No.2) on factor B cleavage was determined by quantitating the limited cleavage of factor B by factor D. C3b (2 μg) was preincubated for 15 minutes at 37°C with different concentrations of the peptide. The reaction mixture was then incubated at 37°C for 30 minutes with 2 μg of factor B and 0.06 ng of factor D in a total volume of 20 μl VBS containing 5 mM MgEGTA. The percentage of factor B cleaved was determined by electrophoresis of samples on a 7.5% SDS-PAGE gel under reducing conditions and densitometric analysis of the stained gel. Controls contained 10 mM EDTA instead of 5 mM MgEGTA.

ELISA for measurement of C3 binding to properdin. Binding of properdin to C3 was determined by ELISA.

Microtiter wells were coated with 50 μl of C3 (20 μg/ml) by incubation at 37°C for 1 hour. After coating, wells were saturated with 200 μl of blocking buffer at 22°C for 30 minutes and incubated 1 hour at 22°C with 50 μl of NHS diluted 1:50 in PBS, pH 7.4, containing 10 mM EDTA. To determine the effect of peptide IV (Sequence I.D. No.2), various concentrations of the peptide were added to the reaction mixture. The amount of properdin bound to C3 was quantitated by adding 50 μl of polyclonal goat anti-properdin antibody (10 μg/ml), followed by 50 μl of peroxidase-conjugated anti-goat antibody diluted 1:1000 in PBS (BioRad, Hercules, CA). Each antibody was incubated at 37°C for 1 hour and washed with PBS, pH 7.4 containing 0.05% Tween 20. Color was developed by adding ABTS peroxidase substrate, and optical density was measured at 405 nm.

***In vivo* clearance of the C3-binding peptide.** A C3 binding peptide of the invention, containing tyrosine residues at its C-terminus (ICVVQDWGHHRCTAGHYY (Sequence I.D. No.23)), was labeled with ^{125}I using Iodogen (Pierce) and purified on a reverse-phase C-8 cartridge (Waters). The labeled peptide had a specific activity of 0.7 μCi/μg. Normal SJL mice were injected via the tail vein with 1.4 μg of ^{125}I-Peptide. Blood samples were withdrawn at various time intervals and the radioactivity was determined, The first sample, taken out immediately after injecting the labeled peptide is referred to as the zero time point.

RESULTS

To identify peptides of the present invention, a phage-displayed random peptide library containing 2 x 10^8 unique clones expressing random peptides 27 amino acids in length was screened. Peptides of this library are fused to the amino terminus of the mature protein III of bacteriophage M13. Because C3b has a relatively low

affinity for other complement proteins, half-physiologic ionic strength buffers have traditionally been used to study these interactions. However, to increase the probability of selecting a phage with high affinity, buffers of physiologic ionic strength for biopanning were used. Phage particles expressing C3b-binding peptides were affinity-purified by plating on a microtiter plate coated with C3b. After a third round of biopanning, individual phage were isolated and tested for binding; 14 of 16 clones bound to C3b. DNA was isolated from all positive clones and the nucleotide sequence of each was determined. All fourteen positive clones had an identical sequence, indicating that this clone was specific and had been amplified during the second and third rounds of biopanning.

Binding results obtained with representative positive (clone 9; Sequence I.D. No.4) and negative (clone 1) clones showed that clone 9 bound to immobilized C3, C3b and C3c but not to C3d (see Figure 1). The binding strength of the positive clone followed the order C3 > C3b > C3c. Specificity of the binding of clone 9 was demonstrated by ELISA. Aggregated C3 (250 μg/ml) significantly inhibited the binding to C3, C3b and C3c.

A 27-amino acid peptide (Sequence I.D. No.1) corresponding to the phage-displayed peptide was synthesized. This peptide, in its cyclic form, is referred to herein as peptide I. The amino acid sequence of peptide I is shown in Table 1. Peptide I was found to bind to C3 and some C3 fragments, inhibiting both classical and alternative pathways of complement activation. The synthetic peptide (peptide I) was coated on a microtiter plate and its binding to C3 and C3 fragments was analyzed by ELISA. Immobilized peptide I bound to C3 and C3b; however, no binding to C3d was detected (Figure 2). Peptide I also did not bind to C3c (Figure 2), thus indicating that the peptide's binding

site is buried when C3c is present in its native conformation.

This peptide inhibits complement activation in normal human serum by inhibiting the proteolytic activation of C3 at a concentration approximately twice that of human C3. Inhibition of the alternative pathway was measured by using rabbit erythrocytes in the presence of MgEGTA (Figure 3A); inhibition of lysis of antibody-coated sheep erythrocytes was used as an indicator of inhibition of the classical pathway (Figure 3B). Peptide I inhibited both classical and alternative pathways with IC_{50} of 65 μM and 19 μM, respectively.

Analysis of the mechanism of inhibition revealed that this peptide inhibited C3 cleavage in normal human serum in the presence of MgEGTA. Similar results were obtained when the alternative pathway was reconstituted with purified complement components. However, the peptide did not inhibit the cleavage of factor B, indicating that it did not affect the interaction of C3b with factor B or the formation of C3b,Bb. The peptide also had no effect on the binding of properdin to C3, demonstrating that the observed inhibition of C3 cleavage in normal human serum was not due in part to its effect on the properdin-stabilized C3 convertase, C3b,Bb,P. These results indicate that, unlike other regulators of complement activation (factor H, MCP, DAF and CR1) that inhibit the activation process subsequent to the generation of C3b, the peptide of the present invention interacts directly with native C3 to inhibit its activation.

Various analogs of peptide I were examined to the determine the region or residues of the peptide involved in inhibition of complement. Results from these experiments are shown in Table 1. The purity and identity of all the peptides were critically monitored by laser desorption mass spectrometry (Moore, W.T. *Biol. Mass Spectrom.* 1993 **22**:149-162). In all cyclic peptides,

formation of a disulfide bond was confirmed mass spectrometrically using a mass shift assay involving reactions of thiols with p-hydroxy mercuribenzoic acid (Angeletti et al. *Techniques in Protein Chemistry VII*. Edited by Marshak DR. San Diego, Academic Press, 1996 p. 261).

Table 1. Amino Acid Sequences and Functional Activity of Compstatin and its Analogs

(N.D. = not done)

PEPTIDE/ CLONE	AMINO ACID SEQUENCE	CLASSICAL PATHWAY IC_{50} (μM)	ALTERNATIVE PATHWAY IC_{50} (μM)
CLONE 9 SEQ ID NO: 4	SSICVVQDWGHHRCTAGHMANLTSHASAIR	N.D.	N.D.
PEPTIDE I SEQ ID NO: 1	ICVVQDWGHHRCTAGHMANLTSHASAI |_____|	65	19
PEPTIDE II SEQ ID NO: 1	ICVVQDWGHHRCTAGHMANLTSHASAI	>300	>300
PEPTIDE III SEQ ID NO: 3	RATAGHMANLTSHASAI	>300	>300
PEPTIDE IV SEQ ID NO: 2 (Compstatin)	ICVVQDWGHHRCT |_____|	63	12
PEPTIDE V SEQ ID NO: 2	ICVVQDWGHHRCT	>600	>300
PEPTIDE VI SEQ ID NO: 13	CVVQDWGHHRC |_____|	N.D.	33
PEPTIDE VII SEQ ID NO: 5	CHHRCT |___|	N.D.	>600
PEPTIDE VIII SEQ ID NO: 6	CGHHRCT |____|	N.D.	>600
PEPTIDE IX SEQ ID NO: 7	CWGHHRCT |_____|	N.D.	>600
PEPTIDE X SEQ ID NO: 8	CDWGHHRCT |_____|	N.D.	>600
PEPTIDE XI SEQ ID NO: 9	CQDWGHHRCT |_____|	N.D.	>600

PEPTIDE/ CLONE	AMINO ACID SEQUENCE	CLASSICAL PATHWAY IC_{50} (μM)	ALTERNATIVE PATHWAY IC_{50} (μM)
PEPTIDE XII SEQ ID NO: 10	CVQDWGHHRCT	N.D.	>600
PEPTIDE XIII SEQ ID NO: 11	CVVQDWC	N.D.	>600
PEPTIDE XIV SEQ ID NO: 12	CVVQDWGHC	N.D.	>600
PEPTIDE XV SEQ ID NO: 14	CAVQDWGHHRC	N.D.	1200
PEPTIDE XVI SEQ ID NO: 15	CVAQDWGHHRC	N.D.	67
PEPTIDE XVII SEQ ID NO: 16	CVVADWGHHRC	N.D.	910
PEPTIDE XVIII SEQ ID NO: 17	CVVQAWGHHRC	N.D.	257
PEPTIDE XIX SEQ ID NO: 18	CVVQDAGHHRC	N.D.	182
PEPTIDE XX SEQ ID NO: 19	CVVQDWAHHRC	N.D.	>1200
PEPTIDE XXI SEQ ID NO: 20	CVVQDWGAHRC	N.D.	15
PEPTIDE XXII SEQ ID NO: 21	CVVQDWGHARC	N.D.	74
PEPTIDE XXIII SEQ ID NO: 22	CVVQDWGHHAC	N.D.	70

To identify the minimal region of peptide I that is required for interaction with C3, two overlapping peptides were synthesized and their activities determined in the classical and alternative pathway-mediated hemolytic assays. See Table 1. The two overlapping peptides tested were the cyclic 13-amino acid N-terminal peptide (peptide IV) and the linear 17-mer C terminal peptide (peptide III). Inhibitory activity was retained

by the cyclic N-terminal region of the parent peptide (peptide IV). In contrast, peptide III showed no inhibitory activity, indicating that this region is not important for binding. In addition, linear peptides II and V were made by reducing and alkylating peptide I and IV, respectively. This reduction and alkylation destroyed the inhibitory activity of peptides I and IV, indicating that the cysteine disulfide bridge is important in maintaining the stable structure of peptide I and IV. The concentration of peptide I or IV that was required to inhibit the alternative pathway was lower than that required to inhibit the classical pathway, perhaps because the alternative pathway is more sensitive to activation and deposition of C3 on the target cells.

Peptide IV, which was re-named "Compstatin," demonstrated the greatest overall complement-inhibiting activity. As shown in Table 1, Compstatin is a 13-residue peptide of 1551 u with sequence (Sequence I.D. No. 2):

Ile^{1}-Cys^{2}-Val^{3}-Val^{4}-Gln^{5}-Asp^{6}-Trp^{7}-Gly^{8}-His^{9}-His^{10}-Arg^{11}-Cys^{12}-Thr^{13}

containing a disulfide bridge between Cys^{2} and Cys^{12}.

Compstatin contains two flanking amino acid residues outside the constrained region. To further reduce the size of the peptide, these two residues were deleted to produce peptide VI. This deletion resulted in approximately 2.8-fold reduction in the activity of the peptide.

An additional series of analogs was synthesized in order to localize the minimal functional region of the peptide. Short constrained peptides were generated by changing the ring size. For this purpose, one to six residues inside the 11-membered ring were deleted (peptides VII-XIV of Table 1). However, activity was lost in all the peptides of this series, indicating that reducing the ring size alters some structural feature of the peptide important for its binding and/or complement-inhibiting activity.

In an additional series of analogs, the contribution of each residue to maintaining biological activity of the peptide was determined by replacing it with an Ala. In this series of nine peptides (peptide XV-XXIII of Table 1), each residue of the 11-membered ring, except for the two cysteines, was systematically substituted with alanine. Replacement of Val^4, His^9, His^{10} or Arg^{11} (based on the numbering system for Compstatin, set forth above) resulted in minimal change in the functional activity, suggesting that these residues may not contribute significantly to the interaction with C3b. Replacement of Val^3, Gln^5, Asp^6 or Trp^7 (again based on the numbering of residues in Compstatin) reduced the activity of the peptide from 6- to 36-fold as compared to peptide VI. These residues are clustered together in the N-terminal half of the peptide. Replacement of Gly^8 with Ala dramatically reduced the activity of the peptide by more than 100-fold, suggesting that the side chain of the Ala may sterically hinder the binding of the peptide to C3, or that the free rotation around glycine is important for binding. Thus, it is believed that the side chains of Val^3, Gln^5, Asp^6 and Trp^7 (Compstatin numbering) contribute significantly to the binding and biological activity of the peptide.

Compstatin has also been determined to inhibit C3 convertase C3b,Bb-mediated cleavage of C3 in a concentration dependent manner (see Figure 4). The peptide inhibited C3 cleavage with an IC_{50} of 10 μM that correlated well with the concentration required to inhibit 50% of the hemolytic activity (Table 1). During complement activation in serum, C3 convertase cleaves C3 into C3b, which is immediately inactivated by factors H and I to iC3b. This assay measures the amount of iC3b generated during activation. Thus, to verify that the measured inhibition was due to inhibition of C3 cleavage by C3 convertase and not to inhibition of factors H- and I-mediated cleavage of C3b to iC3b, 5 μg of purified C3b

was incubated with 1 μg of factor H and 0.04 μg of factor I in the presence of Compstatin. No inhibition of iC3b generation was observed, even at 300 μM, a concentration 30 times higher than the IC_{50} for C3 cleavage.

To examine the effect of Compstatin on purified C3, free of possible labeling artifacts, the alternative pathway was reconstituted with purified C3, factor B and factor D (see Figure 5). Compstatin inhibited the proteolytic activation of C3 to C3b, with an IC_{50} of 28 μM. Peptide V, the reduced and alkylated form of Compstatin, had no effect on C3 cleavage.

The interaction of C3b with factor B in a fluid phase assay in which purified C3b, factor B and factor D were incubated together with MgEGTA so as to generate C3b,Bb in the presence or absence of Compstatin was also determined. The concentration of factor D was adjusted to generate limited cleavage of factor B. Compstatin showed no inhibition of factor B cleavage (Figure 6), indicating that this peptide has no effect on the interaction of C3b with factor B or on C3b,Bb formation.

The effect of Compstatin on properdin binding to C3 was also determined using a competitive ELISA (see Figure 7). Compstatin had no significant effect on properdin binding to C3, indicating that the observed inhibition of C3 cleavage in NHS is not due to disruption of the properdin-stabilized C3 convertase, C3b,Bb,P.

EXAMPLE 2
Retro-inverso Peptidomimetic of Compstatin

Natural L peptides are vulnerable to cleavage by proteolytic enzymes *in vivo*. Therefore, solid-phase peptide synthesis methods were used to make a protease-resistant, retro-inverso peptidomimetic derivative of Compstatin. In the synthesis of this analog, the direction of the sequence is reversed, changing the chirality of each amino acid by using all D-amino acid residues, thereby conferring protease resistance.

Topographically, the D-amino acid side-chain configurations all correspond to the natural all L-form derivative, and activity may be preserved if the orientation of the side chain is the most important aspect of the specific ligand interaction system in question (Chorev, M. and Goodman, M. Trends in Biotech. 13: 438-445, 1993). Recent studies have demonstrated the preservation of the antigenicity of a retro-inverso peptide mimetic derivative of the C-terminus of a histone H3 sequence (Guichard et al. Proc. Nat'l Acad. Sci. USA 91: 9765-9769, 1994) and the transport function of a 16-mer retro-inverso form of a homeobox domain (Brugidou et al., Biochem. Biophys. Res. Commun. 214: 685-693, 1995). However, if instead the main-chain atoms play a significant role in the ligand interaction system, a retro-inverso peptidomimetic analog, along with its consequential change in directionality of the main chain atoms, may be inactive, as found in a recent study on a hormone-binding domain of a vasopressin receptor (Howl, J. and Wheatley, M. Biochem. J. 317: 577-582, 1996). The retro-inverso analog of Compstatin was found to be inactive in the complement-mediated hemolytic assay, indicating that main chain atoms of Compstatin play a significant role in maintaining the preferred structure of the peptide.

EXAMPLE 3
Use of Synthetic Peptide Chemistry with Mass Spectrometric Validation to Design Additional Analogs of Compstatin

In this Example we describe the use of synthetic peptide chemistry with mass spectrometric validation of structure to provide a series of substitution analogs that are rationally designed to exaggerate broad chemical properties of Compstatin. Variants are constructed by substituting conservative or non-conservative residues to modify properties such as hydrophobicity, acidity, basicity or the bulkiness of a residue side chain.

Substitution analogs. Substitution analogs are designed to exploit critical residue positions established by the analogs described in Example 1. In the design of additional synthetic peptides, residues are substituted that increase homologous or heterologous chemical properties of the amino acid side chain, such as hydrophobicity, while having only minimally impact on the bulkiness of the side chain. For example Val' is replaced with Ile, Leu or Thr. These substitutions are in keeping with either hydrophobicity (I and L) or in side-chain bulkiness with a change toward hydrophilicity (T). Gln' is substituted with Asn, Glu, Lys or Met. An Asn substitution preserves the electrical neutrality with a change toward less bulkiness, a Glu introduces a negative charge at this critical site, preserving the side chain bulkiness, and also tests the question of whether deamidation is problematic in the minimal-structure Compstatin molecule. Lysine introduces a basicity at this site while preserving the side-chain bulkiness and is a good candidate, since this substitution -although perceived as chemically non-conservative- is often observed in nature. A Met introduces some hydrophobicity into this area while preserving side-chain bulkiness and creates a site that is modifiable by oxidation. Asp' is replaced with Glu to preserve the acid function in this area while increasing side chain bulkiness, with Asn to neutralize the charge and preserve side-chain bulkiness. Trp' is substituted with a Tyr to preserve polarity and to maintain partially the bulky side-chain ring-structure present in this position; with a His to retain polarity and the partial ring-structure character of the side-chain; and with a Phe to introduce hydrophobicity and to partially maintain the bulky side-chain ring structure. The Gly' position appears to be unique in that any addition in side-chain bulkiness in this area compromises activity and cannot be tolerated. It appears as though the conformational freedom offered by Gly in this

position is a requirement for activity. The minimal increase in bulkiness in this area is afforded by an Ala substitution, with the side chain hydrogen of Gly is substituted by a methyl group. As described elsewhere herein, substitution of Ala for Gly resulted in a significant loss of activity, supporting the notion that the conformational freedom afforded by Gly is needed for activity. However, this could be further explored by making derivatives substituted in Ser, Val and Leu. These residues represent the residues with the least side-chain bulkiness after Ala.

As for the putative non-critical sites, Val^{4}, His^{10} and Arg^{11}, this region can be further characterized by making Pro substitutions, individual deletions and all-Gly or-Ala substitutions. Proline has a disruptive character in that it offers the least amount of conformational freedom in a polypeptide chain because the side chain is fixed to the main chain by a covalent bond. Attempts at ring-size reduction (see Example 1) suggest that deletions in ring size are not tolerated. The derivatives mentioned above and analogs with all positions simultaneously substituted with residues having minimally contributing side chains, such as Gly, can be examined as one way to determine whether these sites are totally non-critical.

All the aforementioned derivatives can be assayed *in vitro* in a hemolysis assay as described in Example 1. For the most potent derivatives, the *in vivo* half-lives can be measured using a Tyr-containing derivative that is inserted in a version having a C-terminal extension that is biologically irrelevant.

Chemical modification analogs. To obtain additional informative analogs of Compstatin, covalently modified versions are prepared and evaluated for *in vitro* and *in vivo* reactivity. Most of the chemistry exploits the reaction of nucleophilic sites offered by certain

side chains with electrophilic reagents. With the N-acetylation of the N-terminus and C-termini existing in the amide form and the given constituent residues, all chemical modification chemistries will result in residue-specific modifications with little modification of other residues. All modification chemistries and purified products are evaluated by mass spectrometry for validation of structure, and only those products that are clearly characterizable are assayed and further analyzed. Modified peptides are prepared by post-synthetic chemical modification chemistries of intact peptides and also by incorporating modified amino acids in a synthetic run (Means & Feeny, Chemical Modification of Proteins, Holden-Day, Inc., 1971).

1) ***Post synthetic modifications***

Asp' Modification: If the Compstatin is synthesized with a C-terminal amide, Asp' offers a single carboxyl group for modification. Aspartamide is induced at this position during a synthetic run. In this reaction the β carboxyl of the Asp undergoes nucleophilic attack by the α N and forms a cyclic amide ring (Bodansky & Martinez, in The Peptides, Gross & Meinhofer, eds., NY Academic Press, 111-216, 1981). This modification adds additional constraint to the structure while neutralizing a negative charge. This carboxyl group can also be esterified to form a methyl ester by the reaction of the peptide with methanolic HCl. This modification neutralizes the negative charge and increases the hydrophobicity at this position. Two other reactions can be performed at this site using a water soluble carbodiimide to activate the beta carbonyl for reaction with the nucleophile taurine that has an amine function at one end (that will couple to the activated carboxyl) and a sulfate moiety at the other end (that will introduce a highly negatively charged sulfate group at the site with an increase in side chain bulkiness). Reaction of the water soluble carbodiimide activated

carbonyl with diamine allows a similar change in the increase in side chain bulkiness with the introduction of a basic function that will be positively charged at physiological pH.

Trp' Modification: Two modifications are selected for Trp'. The first entails the reaction of the peptide with 2-((2-nitrophenyl)sulfenyl)-3-methyl-3'-bromoindolenine (BNPS-skatole) (Omenn et al., J. Biol. Chem. 245: 1895-1902, 1970). If this reaction is performed in a controlled fashion, the indole moiety of the Trp becomes oxidized to oxindole thereby slightly increasing the polarity of this region of the peptide without extensively modifying the bulkiness of the side chain group. This reaction must be carefully monitored by mass spectrometry since extensive reaction can lead to cleavage of the chain at the Trp site. Reaction of the peptide with 2,4-dinitrobenzenesulfenyl chloride will introduce a dintitro benzene moiety to the indole moiety greatly increasing the bulkiness of the indole side chain (Scoffone et al., Biochem. 7: 971-979, 1996). This reaction is an electrophilic substitution reaction at the carbon 2 of Trp.

His^{9,10} modifications: The modification of His^{9,10} upon iodination will be explored because this chemistry has a significant relevance to the biological activity of ^{125}I-Compstatin radioligands. It is well established that both mono and diiodohistine are formed under some iodination conditions (high pH) even though the reactivity of this moiety is perceived much less than that of the phenol group of Tyr. The addition of iodine atoms to the imidazole ring slightly increases the bulkiness of the side chain. Iodogen is preferable for use an oxidizing reagent to generate reactive iodine, for the purpose of assessing possible consequences that may be encountered in the preparation of radioiodinated Compstatin. The harsher oxidizing reagent, chloramine T, can also be employed, and the ICl method at alkaline pH's

to drive the reaction toward His and to assess consequences of extensive modification of this residue (Means & Feeny, 1971 *supra*). Other possible side effects of this chemistry, such as the oxidation of Trp, can be monitored using mass spectrometric techniques. The pH dependent (pH < 8) reaction of His with iodoacetamide can also be exploited (Schnackerz & Noltmann, J. Biol. Chem. 245: 6417, 1970). The result of this reaction is to incorporate a carboxamido group to one of the imidazole moiety nitrogens, modifying the basicity and bulkiness of this side chain. Acetic anhydride diethyl pyrocarbonate, a reagent that has shown the greatest selectivity toward Histidine if the reaction is run a pH slightly below the pKa of the reagent, can also be employed (Miles, Meth. Enz. 47: 431-442, 1977). This chemistry adds an ethoxycarbonyl group to the His at the same side chain site as the previously described chemistry and also alters the basicity of the imidazole with a further increase in bulkiness.

Arg" modifications: Arginines may be specifically modified with vicinal diones such as cyclohexanedione (Carlson & Preiss, Biochem. 21: 1929, 1982). This modification is thought to result in the introduction of bulky ring-structures at the end of the guanidino moiety of this side chain.

2) ***Presynthetic modification using commercially available modified FMOC amino acids***

Compstatin analogs can also be synthesized utilizing modified FMOC protected amino acids that reflect some observed *in vivo* post-translational modifications. Some of these changes will alter protease sensitivity and may effect *in vivo* biological activities. The following FMOC amino acids are available for preparing chemically modified analogs: 3-carboxyaspartate at the Asp' position using FMOC-Gla(OtBu),-0H (Bachem # B1265), N-methyl Asp at the Asp'

position using FMOC-N Me-Asp (Peptides International # FMD1890-PI), dimethyl-Arg at the Arg[11] position using FMOC-Arg(Me)2-OH (Bachem# B-2745) and N-methyl Valine at either Val[3] or Val[4] or both positions using Fmoc-N-Me-Val (Peptides International # FMV-1796-PI).

Constrained cyclic analogs. We have observed that reduction and alkylation with iodoacetamide destroys Compstatin activity (Example 1). We conclude from this experiment that the presence of the disulfide is necessary for activity, presumably to preserve a constrained backbone structure within the peptide. However, it should be noted also that the alkylation step introduced bulky carboxamido methyl groups onto the sulfur atom in each Cys. To confirm that the analog needs to be cyclic (or to have its constrained backbone structure preserved by some other means) for optimal activity, a derivative incorporating the residue Abu (aminobutyric acid) at the Cys positions can be constructed. Abu has a methyl group in the position where the thiol would exist in cysteine and therefore is an excellent isosteric substituent for Cys. Substitution of this residue in bovine pancreatic trypsin inhibitor did not interfere with the folding of the molecule (Ferrer et al., Int. J. Pept. Protein Res. 40: 194-207, 1996), indicating that cysteines do not drive folding but probably stabilize the optimal folding pattern after it occurs. It is possible that a Compstatin Abu derivative may show some activity. However, constraint of peptide conformation in solution has led to higher potency in some bioactive peptides (Sawyer et al., Proc. Natl. Acad. Sci. USA 79: 1751-1755, 1982). If Abu-derivatization reveals that conformational constraint is a requirement for optimal activity of Compstatin, other means of constraint can be introduced through peptide cyclization, such as through the N-terminal α-amino group and the C-terminal α-carboxyl group of an Abu[2,12] derivative or side

chain ϵ-amino group of a Lys' derivative and the side-chain terminal carboxyl of α Glu'' or Asp'' side-chain derivative. To increase constraint parameters while taking advantage of thiol oxidation chemistry that we can carefully monitor and validate through mass spectrometric analysis using PHMB (Angeletti et al., 1996 *supra*), Compstatin peptides can be made with Cys positions substituted with penicillamine (Pen, B,B-dimethyl-cysteine). The two methyl groups added to the side chain β carbon add a further conformational constraint to the disulfide formed from these residues and, in some instances, have increased the potency of bioactive peptides. The following derivatives can be prepared:

Compstatin: ICVVQDWGHHRCT
|_____|

#1: IKVVQDWGHHRET
|____NCO__| (NCO represents a peptide bond)

#2: IabuVVQDWGHHRAbuT

#3: (HN-Abu)VVQDWGHHR(Abu-CO)
|_____|

#4: IpenVVQDWGHHRCT
|_____|

#5: IpenVVQDWGHHRPenT
|_____|

#6: ICVVQDWGHHRPenT
|_____|

EXAMPLE 4
Targeted Random-Peptide Phage Library Constructs

In addition to the solid-phase peptide synthesis approach using chemical modification to generate a diverse collection of analogs, we will also design and screen two random-peptide phage libraries with diversity limited to specific regions of the peptide that have already been deemed structurally significant for bioactivity from the previous studies. The libraries are modelled after the following constructs:

Base model of Compstatin: ICVVQDWGHHRCT
|_____|

Library 1: XCVXXXXGHHRCX
|_____|

Library 2: XCVVQDWXXXXCX
|_____|

Screening of the targeted phage library is performed as described in Example 1. In brief, microtiter wells (Nunc Inc., Naperville, IL) are coated with C3b in phosphate buffered saline (PBS) and blocked with PBS containing BSA. After washing, 6 x 10^{11} plaque forming units of these libraries are added to each well and incubated overnight at 4 °C. The wells are washed with PBS containing 0.1% tween 20 and 0.1% BSA. Bound phage particles are either eluted with glycine-HCl, pH 2.3 or with a specific ligand (C3). Phage particles eluted with glycine-HCl are immediately neutralized with Tris-HCl, pH 8.5. Recovered phage particles are amplified in *E. coli* cells. Biopanning procedure are repeated twice to enrich the specific clones. To select for high affinity binders, the clones are re-screened from the first screening by using, in the different washing steps, varying amounts of NaCI (150-500 mM). Representative clones are sequenced and the corresponding

peptides synthesized and tested for their ability to inhibit complement activation.

EXAMPLE 5

Determination of Solution Structure of Compstatin

Small peptides are in most cases present in solution as an ensemble of interconverting conformers. In some cases the population of one or more conformers in the ensemble can be high enough for detection by spectroscopic methods. Cyclic peptides are more restrained in flexibility as compared to linear peptides, and they are more likely to demonstrate a preference for an observable conformer. The presence of rapidly interconverting conformers is reflected in the measured NMR parameters, which are population-weighted averages of the individual contributing structures.

In the present example we have used NMR spectroscopy to extract distance, dihedral angle and $^3J_{NH-H\alpha}$-coupling constant restraints (Wüthrich, NMR of Proteins and Nucleic Acids; John Wiley Sons, New York, 1986), which we have used for the structure elucidation of a major Compstatin conformer. We utilized a hybrid distance geometry-restrained simulated annealing methodology (Nilges et al., FEBS Lett. 229: 317-324,1988; Nilges et al., in Computational Aspects of the Study of Biological Macromolecules by NMR (J.C. Hoch, ed.) Plenum Press, NY, 1991; Kuszewski et al., J. Biomol. NMR 2: 33-56, 1992) for the structure calculation. Subsequently, we examined the structure for consistency using characteristic NOE connectivities, $^3J_{NH-H\alpha}$-coupling constants, chemical shifts and temperature dependence of chemical shifts (Wüthrich, 1986 *supra*; Dyson et al., FASEB J. 9:37-42, 1988). In addition, we analyzed the contribution of each amino acid residue by synthesizing and examining the inhibitory activity of a series of analog peptides with Ala substitutions. The analog data, together with the 2D NMR data, indicate that the C3

binding site is formed by the type I β-turn segment (Gln^5-Asp^6-Trp^7-Gly^8) in Compstatin.

MATERIALS AND METHODS

Peptide synthesis, purification and characterization. Compstatin (peptide IV) and its analogs were synthesized in an Applied Biosystem peptide synthesizer (model 431A) using Fmoc amide resin, as described in Example 1.

Complement inhibition assays. Inhibition of complement function by Compstatin and analog peptides was studied by measuring their effect on the alternative pathway of complement, as described in Example 1.

NMR sample preparation. The NMR samples were prepared by dissolving Compstatin in 0.6 ml of 90% H_2O-10% D_2O containing 0.05 M potassium phosphate, 0.1 M potassium chloride, 0.1% sodium azide and 10^{-5} M EDTA. Compstatin is highly soluble in aqueous solution; solvation to a final concentration of 3 mM was instantaneous. Mass spectroscopy showed the solution to be monomeric. The sample, prepared at pH 6 was highly pure and suitable for NMR spectroscopy. pH 6 was chosen because it is lower than the pH favoring cysteine oxidation-reduction reactions and higher than that which favors hydrolysis at the aspartic acid position. This pH was sufficient to achieve slow amide proton exchange with the solvent in order to facilitate the proton assignments. As assessed by mass spectroscopy and one-dimensional NMR spectra, the sample was stable over the period of several days required to collect the 2D NMR spectra. Experiments were performed at 5° C to slow down the peptide tumbling time and to limit potential exchange between the various peptide conformers and amide proton exchange with the solvent.

NMR data acquisition. NMR spectra of Compstatin were acquired with a Varian Unity-plus 500 MHz spectrometer. Standard methods were used to obtain 1D and 2D ^{1}H NMR spectra. These included 2D total correlation spectroscopy (TOCSY) (Braunschweiler and Ernst, J. Mag. Res. 53: 521-528, 1983), 2D double quantum filtered correlated spectroscopy (DQF-COSY) (Rance et al., Biochem. Biophys. Res. Commun. 117: 479-485, 1983), 2D double quantum spectroscopy (DQ) (Braunschweiler et al., Mol. Phys. 48: 535-560, 1983), 2D nuclear Overhauser enhancement spectroscopy (NOESY) (Kumar et al., Biochem. Biophys. Res. Commun. 95: 1-6, 1980), 2D jump-and-return NOE spectroscopy (J-R NOESY) (Plateau and Guéron, J. Am. Chem. Soc. 104: 7310-7311, 1982) and rotating frame NOE spectroscopy (ROESY) (Bothner-By et al., J. Am. Chem. Soc. 106: 811-813, 1984). Experiments were performed at 5°C and repeated at 10°C. Experimental constraints for structure calculations were extracted from the 5°C spectra. Mixing times were 50, 100, 150, 200 and 400 ms for the NOESY, 150 and 200 ms for the J-R NOESY, 60 ms for the TOCSY and 100 and 150 ms for the ROESY experiments. The excitation period for the DQ experiments was 40 ms.

Typical 2D data sets consisted of 2048 or 4096 complex t_2 data points and 400-512 (900-1024 for DQ) complex t_1 data points. The States method (States et al., J. Mag. Res. 48:286-292, 1982) was used to achieve quadrature detection in t_1. A total of 32 scans were averaged for each t_1 experiment. The transmitter carrier was placed at the water resonance in all experiments. A recycling delay of 2 s between scans was used, during which a low power water presaturation was applied for 1 s. Spin locking in the TOCSY experiment was achieved using a DIPSI-2 sequence (Shaka et al., J. Mag. Res. 274-293, 1988). A CW spin lock was used during the ROE mixing time, with an rf field strength of about 4 kHz. The spectral widths were set to 8 kHz in t_2 and to 6.5 or

8 kHz in t_1, with the exception of the DQ experiments, for which the spectral widths were set to 8 kHz and 16 kHz in t_2 and t_1, respectively.

Data processing. Data were processed using the software package FELIX 2.3 (Biosym Technologies, San Diego, CA) on an SGI Indigo workstation. Typically $1024(\omega_1)\times4096(\omega_2)$ real matrices were generated during processing. The residual water signal was removed from the spectra by applying a low frequency filter to the time domain data (Marion at al., J. Mag. Res. 84: 425-430, 1989). The first data point was back linearly predicted in both the t_2- and t_1-dimensions to reduce t_2- or t_1-ridges. Zero filling was applied in the t_1-dimension and in some instances in the t_2-dimension. Removal of a baseline offset was applied to the t_2-time domain spectra using the average value calculated from the last 20% of each free induction decay signal. A 90°-shifted and a 70°-shifted sine bell window function was applied in the t_2- and t_1-dimensions, respectively.

Conversion of NMR parameters to structural restraints. Cross-peak volume integrations were performed with the program FELIX 2.3, using mainly the 150 ms 2D NOESY experiment collected at 5°C. The NOE volumes were then converted to distance restraints after they were calibrated using known fixed distances of the Trp^7 ring. The cross peaks corresponding to NH^{ε}-CH^{δ} and NH^{ε}-$CH^{\zeta 2}$ NOEs of Trp^7 were used as reference for the calibration within the program FELIX 2.3. Then an NOE restraint file was generated with four distance classifications, as follows: strong NOEs (1.8 Å$\leq r_{ij} \leq$2.7 Å, where 1.8 Å is the Van der Waals radius and r_{ij} the interproton distance between protons i,j), medium NOEs (1.8 Å$\leq r_{ij} \leq$3.3 Å), weak NOEs (1.8 Å$\leq r_{ij} \leq$5.0≤ Å) and very weak NOEs (3.0 Å$\leq r_{ij} \leq$6.0 Å). The upper boundary of NOEs involving amide protons was extended to 2.9 Å for strong

NOEs and to 3.5 Å for medium NOEs to account for the higher observed intensity of this type of cross peak (Qin et al., Structure 4: 613-620, 1996). In addition, a 0.5 Å correction (Qin et al., 1996 *supra*) was added to the upper boundary of the distances involving methyl groups to account for the averaging of the three methyl protons. An NOE restraint between the two sulfur atoms of Cys^2 and Cys^{12} was set during the distance geometry calculation, corresponding to distance 2.02 Å. During structure calculations distances involving non-stereo-specifically assigned or degenerate methylene protons and methyl groups were incorporated as $(\Sigma\ r^{-6})^{-1/6}$ effective distances (Nilges, Protein: Struct. Funct. Genet. 17: 297-309, 1993). A total of 136 NOE-derived distance restraints were used, 83 intra residue, 30 backbone-backbone or H^{β}-backbone and 23 medium and long range, corresponding to an average of 10.5 NOEs per residue.

Resolved β-methylene protons were observed only for residues His^9, Arg^{11} and Cys^{12}. Resolved methyl protons were observed for residues Ile^1 and Val^4. Stereospecific assignments were made for the β-methylene protons of His^9 and Cys^{12}. Side chain χ_1-dihedral angles for the residues involving stereospecific β-methylene proton assignments were restrained to one of the staggered conformations. In the case of His^9 and Cys^{12} the value was found to be $\chi_1=-60°\pm30°$, using the combined information from H^{α}-H^{β} DQF-COSY cross-peak patterns and NOE intensities of NH-H^{β} cross peaks.

$^3J_{HN-H\alpha}$-coupling constants were measured from the 2D DQF-COSY spectrum. For accurate evaluation of coupling constants the data were processed without window function weighting, and they were zero filled to 16K points in the t_2-dimension. Traces for 11 backbone NH-H^{α} cross peaks were selected along ω_2. Their antiphase absorptive and dispersive peak-to-peak separations were measured and fitted to Lorentzian line shapes in order to extract $^3J_{HN}$.

$_{H\alpha}$-coupling constants according to the method of Kim and Prestegard (1989 *supra*). Two additional procedures were used for evaluation of coupling constants from the same data set using the NMR data processing program FELIX 2.3. The first procedure consisted of a manual selection of the four peak extrema of each DQF-COSY cross peak and measurement of the peak-to-peak separations of the upper and the lower cross peak lobes (Felix 2.3 manual, 1994). However, the values obtained were very unstable and dependent upon the way the four peak centers were selected. The second procedure involved specification of the footprint of a DQF-COSY cross peak, separation of the upper and lower cross peak lobes, one-dimensional projection of all rows within the lobe and peak-fitting to Gaussian lineshapes (Felix 2.3 manual, 1994). This procedure broke down for Trp^7, His^{10} and Cys^{12}. The three different methods for evaluating coupling constants and the raw peak-to-peak separation yielded values within 1 Hz of each other. The calculated coupling constants and their estimated error of 1 Hz were used for direct J-coupling refinement in the final stages of the peptide structure calculation (*vide infra*).

Dihedral angles were calculated using the J-values extracted from the Kim and Prestegard method (1989 *supra*) by solving the Karplus equations (Karplus, J. Chem Phys. 30: 11-15, 1959; Bystrov, Prog. Nucl. Magn. Res. Spectrosc. 10: 40-81, 1976) with coefficients A=6.98, B=-1.38, C=1.72 (Wang and Bax, J. Am. Chem. Soc. 118: 2483-2494, 1996). Only ϕ-angles that correspond to $^3J_{NH-H\alpha}$-coupling constants that yielded only two real roots for ϕ when the Karplus equations were solved (Karplus, 1959 *supra*). Specifically, for $^3J_{NH-H\alpha} \geq 9$ Hz a dihedral angle of $\phi=-120°\pm40°$ was used and for $7.9 \leq {}^3J_{NH-H\alpha} < 9$ Hz a dihedral angle of $\phi=-120°\pm50°$ was used. The range was calculated to be $\pm20°$ and $\pm30°$ for the two categories, respectively, in order that both solutions of the Karplus equations would be covered with an additional $\pm20°$ as an

error. For $^3J_{NH-H\alpha} \leq 7.3$ Hz, no ϕ-angle restraint was used, since all four solutions of the Karplus equations are possible for a turn segment. However, during the direct $^3J_{NH-H\alpha}$-coupling constant minimization we used all evaluated $^3J_{NH-H\alpha}$-coupling constants and no ϕ-angle restraint.

A total of 7 (out of 12 calculated) ϕ-dihedral angle, 2 χ_1-dihedral angle and 12 $^3J_{NH-H\alpha}$-coupling constant restraints were used. The 7 ϕ-angles, corresponded to Cys^2, Val^3, Trp^7, His^9, His^{10}, Cys^{12}, Thr^{13}. The $^3J_{NH-H\alpha}$-coupling constants corresponded to all residues except Ile^1. The $^3J_{NH-H\alpha}$-coupling constant of Cys^2 was estimated from the 1D ^1H NMR spectrum.

Structure calculations. The Compstatin structures were calculated using the hybrid distance geometry-simulated annealing and refinement protocol (Nilges et al., 1988 *supra*; Nilges et al., 1991 *supra*; Kuszewski et al., 1992 *supra*), with further direct $^3J_{NH-H\alpha}$-coupling refinement (Garrett et al., J. Mag. Res. B 104: 99-103, 1994) using the program X-PLOR 3.851 (Brünger, X-PLOR version 3.1, Yale University Press, 1992). The minimized target function during simulated annealing was composed of quadratic harmonic potential terms for covalent geometry (bonds, angles, planes, chirality), a quartic Van der Waals repulsion term for the non-bonded contacts, quadratic square-well potentials for the experimental distance and dihedral angle restraints and harmonic potential for the $^3J_{NH-H\alpha}$-coupling constant restraints (Brünger, 1992 *supra*; Garrett et al., 1994 *supra*). No hydrogen bonding, electrostatic or 6-12 Lennard-Jones empirical potential energy terms were present in the simulated annealing target function. A standard quadratic target function was minimized during distance geometry (Brünger, 1992 *supra*).

The input force constants for bonds, angles, planes and chirality were 1000 kcal mol^{-1} $Å^{-2}$, 500 kcal mol^{-1} rad^{-2}, 500 kcal mol^{-1} rad^{-2} and 500 kcal mol^{-1} rad^{-2},

respectively and 4 kcal mol^{-1} $Å^{-4}$ for the quartic Van der Waals repulsion term. The input NOE, dihedral angle and $^3J_{HN-H\alpha}$-coupling constant force constants were 50 kcal mol^{-1} $Å^{-2}$, 200 kcal mol^{-1} rad^{-2} and 1 kcal mol^{-1} Hz^{-2}, respectively. Force constants were varied during the various steps of the structure calculation according to the standard X-PLOR protocols (Brünger, 1992 *supra*).

A total of 100 structures were generated, and those with low energies and with no NOE violation > 0.3 Å, no dihedral angle violation > 5°, no bond violation > 0.05 Å, no angle violation > 5° and no improper angle violation > 5° were accepted. The accepted NOE and dihedral angle refined structures were then subjected to further minimization using NOE, χ_1-dihedral angle and $^3J_{NH-H\alpha}$-coupling constant restraints but not ϕ-dihedral angle restraints. This procedure was repeated iteratively to evaluate more distance restraints. A family of structures with similar geometries in the Gln^5-Gly^8 region was observed and the best structure with low energy terms and no $^3J_{NH-H\alpha}$-coupling constant violation > 1.2 Hz was selected for further final refinement.

RESULTS AND DISCUSSION

NMR assignment and restraints. Proton resonance assignments were made according to standard procedures (reviewed in Wüthrich, 1986 *supra*).

Amino acid spin systems were identified by locating networks of characteristic connectivities in the 2D TOCSY spectrum at 5°C. Figure 8 shows the assignment of all thirteen spin systems of Compstatin. The NH of Ile^1 is not observable because of fast exchange with the solvent, but the rest of the spin system is shown at $\omega_2=\omega_{H\alpha}$ (right panel of Fig. 8). In addition, the DQ spectra were very useful for resolving ambiguities and verifying the proton assignments. In particular a remote cross peak was observed in the DQ spectrum at $\omega_2=\omega_{NH}$ and $\omega_1=\omega_{H\alpha1}+\omega_{H\alpha2}$ for Gly^8. This cross peak confirmed the

assignment of the two degenerate α-protons of Gly^8 and resolved the ambiguity at $\omega_2=\omega_{NH}=8.47$ ppm, which is the frequency of the three amide protons (Gln^5, Gly^8, Arg^{11}). Raising the temperature to 10°C introduced small shifts in the resonances of NH protons, a change which allowed us to verify all assignments. Table 2 summarizes the proton assignments of Compstatin at 5°C. The presence of two degenerate methylene protons was verified by observing a remote cross peak in the DQ spectrum at $\omega_2=\omega_{H\alpha}$ and $\omega_1=2\omega_{H\beta}$ (Asp^5, Gln^6, Trp^7, His^{10}), $\omega_2=\omega_{H\beta}$ and $\omega_1=2\omega_{H\gamma}$ (Gln^6, Arg^{11}), and $\omega_2=\omega_{H\delta}$ and $\omega_1=2\omega_{H\gamma}$ (Arg^{11}). Furthermore, the β-protons and the γ-protons of Gln^5 and Arg^{11} were distinguished from each other using step-wise remote and direct connectivities in the DQ spectrum.

Table 2. ^{1}H-NMR chemical shifts (ppm) of Compstatin (pH 6.0, 278 K)[a]

Residue	NH	H^{α}	H^{β}	H^{γ}	H^{δ}	Other
Ile[1]	-	3.89	1.95	1.46, 1.19	0.89	0.97($C^{\gamma}H_3$)
Cys[2]	8.86	4.86	3.06, 3.06			
Val[3]	8.79	4.20	2.07	0.91, 0.91		
Val[4]	8.41	3.87	1.93	0.86, 0.80		
Gln[5]	8.47	4.26	1.70, 1.70	2.18, 2.18		7.41, 6.82 ($H^{\varepsilon 2}$)
Asp[6]	8.34	4.56	2.67, 2.67			
Trp[7]	7.94	4.57	3.30, 3.30			7.25($H^{\delta 1}$), 10.19($H^{\varepsilon 1}$)
						7.46($H^{\zeta 2}$), 7.22($H^{\eta 2}$), 7.15($H^{\zeta 3}$), 7.55($H^{\varepsilon 3}$)
Gly8	8.47	3.72, 3.72				
His[9]	8.28	4.61	3.27($H^{\beta 2}$), 3.03($H^{\beta 3}$)			7.22($H^{\delta 2}$), 8.47($H^{\varepsilon 1}$)
His[10]	8.59	4.62	3.19, 3.19			7.18($H^{\delta 2}$), 8.43($H^{\varepsilon 1}$)
Arg[11]	8.47	4.40	1.82, 1.71	1.55, 1.55	3.13, 3.13	7.24(H^{ε}), 6.89, 6.48(H^{η})
Cys[12]	8.71	4.80	3.22($H^{\beta 2}$), 2.98($H^{\beta 3}$)			
Thr[13]	8.43	4.33	4.23	1.17		
C.T. NH_2	7.75, 7.28					

[a]Chemical shifts reported here are measured in the ω_2-dimension of a 2D NOESY spectrum to ensure best digital resolution, and they are accurate to ±0.01ppm.

Inspection of the 2D NMR spectra indicated the presence of a set of cross peaks corresponding to the backbone of a single Compstatin conformation. However, the results obtained for some side chains, such as Gln^5 and Trp^7 indicated the presence of additional minor conformations. Measurement of the volumes of the NH^{ε} diagonal peaks of Trp^7 in the 2D NOESY spectrum indicated that the Trp^7 ring populated four different conformations with population of 96% for the major side chain conformer and 4% for the rest. No inter- or intra-residue NOEs involving the minor side chain conformations were found, and no conformational exchange cross peaks were found in the ROESY spectrum. For the rest of our analysis we used the unique backbone cross peaks and the cross peaks of the major side chain conformer of Gln^5 and Trp^7.

Sequence-specific and long range NOE assignments were made using the 150, 200 and 400 ms NOESY and the 200 ms J-R NOESY spectra collected at 5° C and 10° C. The J-R NOESY was particularly useful for detecting NOEs involving the α-protons of Cys^2 and Cys^{12} which are very closed to the resonance of water and are "bleached out" by the water suppression scheme of the regular NOESY pulse sequence. 2D ROESY spectra of Compstatin were used to verify the regular NOE assignments that had been made using the 2D NOESY and J-R NOESY spectra.

Figure 9 shows the $^3J_{HN-H\alpha}$ coupling constants of residues Val^3-Thr^{13} that were measured from the DQF-COSY spectrum at 5°C. The data were analyzed using four different methods (described in Materials and Methods). The increased line widths at 5°C did not allow for an accurate evaluation of the $^3J_{HN-H\alpha}$-coupling constants. The method of Kim and Prestegard (1989 *supra*) appeared to be the most robust for calculating $^3J_{HN-H\alpha}$-coupling constants. Still, comparison to direct peak-to-peak separation from in-phase resolved peaks of 1D spectra suggested that the $^3J_{HN-H\alpha}$-coupling constants measured from the 2D DQF-COSY

spectrum gave only the upper limits of the actual values. $^3J_{HN-H\alpha}$-coupling constants are overestimated when they are measured from a 2D DQF-COSY spectrum, due to partial cancellation of the anti-phase COSY cross peak components. Similarly, $^3J_{HN-H\alpha}$-values are underestimated when measured from resolved peaks in 1D spectra because of partial addition of the in-phase 1D peak components. The effect of partial cancellation and addition is more pronounced at 5°C, when the line widths of the NMR signals are broad. This effect was most obvious in the case of the NH-H^{α} peaks of Cys^2, Trp^7, His^9, His^{10} and Cys^{12}. The Kim and Prestegard methodology (1989 *supra*) only partially takes care of the broad line width problem, mainly because of the difficulty in measuring the peak-to-peak separation of the dispersive COSY cross peaks. In general, when the Kim and Prestegard method is used, $^3J_{HN-H\alpha}$-coupling constants of cross peaks with large line widths can be overestimated by up to 1 Hz for line widths that are up to twice as large as the actual $^3J_{HN-H\alpha}$-coupling constant (Kim and Prestegard, 1989 *supra*). A 1 Hz deviation of the measured $^3J_{HN-H\alpha}$-coupling constant corresponds to about ±10° angular deviation. However, deviations of 1Hz need to be examined cautiously at ~7.3 Hz, which is the border value for producing two or four real solutions when solving the Karplus equations. For this reason only $^3J_{HN-H\alpha} \geq 8$ Hz were considered accurate enough to be converted into ϕ-dihedral angles. Such was the case of Cys^2, Va^{13}, Trp^7, His^9, His^{10}, Cys^{12} and Thr^{13} in Compstatin (Figure 9).

Structure calculations. Figure 10, left panel, shows the backbone and the disulfide bond of the ensemble of the 21 accepted, refined structures (out of 30 calculated) for Compstatin. The acceptance criteria were: no NOE violation > 0.3 Å; no angle, dihedral or improper angle violation > 5°; and no bond violation > 0.05 Å. A turn segment was observed in the best-defined

region between residues Gln^5-Gly^8. Figure 10, center panel, shows the backbone of the average restrained regularized structure of the ensemble for the segment Gln^5-Asp^6-Trp^7-Gly^8. The number of NOE restraints per residue, which was used for the structure calculation, is shown in Figure 11, upper panel. The average RMSD of the ensemble of 21 structures for Compstatin was 0.6 Å for the backbone heavy atoms and 1.2 Å for all heavy atoms. The RMSD of the backbone and side chain heavy atoms for each residue of the ensemble of structures is plotted in Figure 11, center panel. The turn segment and the two valines, Val^3 and Val^4, appeared to be better defined than the rest of the peptide. This difference is due to the lack of a significant number of long-range NOE constraints outside the segment Val^3-Gly^8 (Fig. 11, upper panel). The statistics for the ensemble of the family of structures and for the average regularized structure in Figure 10 are summarized in Table 3. The program PROCHECK-NMR (Laskowski et al., J. Biomol. NMR 8: 477-486, 1996) was used for structure validation and analysis. We found that 90% of the residues lay in the most favored or additionally favored regions of the Ramachandran plot (Ramachandran et al., J. Mol. Biol. 7: 95-99, 1963). Only Gln^5 was located in the generously allowed near the border with the additionally allowed regions (Laskowski et al., 1996 *supra*) of the Ramachandran plot.

Table 3. Structural statistics for the ensemble of the family of the 21 final refined structures and the restrained regularized mean structure of Compstatin.

Structural statistics	⟨*Compstatin*⟩	$(\overline{Compstatin})_r$
Experimental RMS deviations		
NOE-derived distance restraints (Å)	0.044±0.003	0.053
Dihedral angle restraints (°)	0.46±0.35	0.21
Deviations from idealized geometry		
Bonds (Å)	0.003±0.0003	0.003
Angles (°)	0.55±0.04	0.55
Improper angles (°)	0.33±0.03	0.34
Potential energies (kcal mol^{-1})		
Total	38.9±5.5	43.3
NOE restraints	13.0±1.9	18.9
Dihedral angle restraints	0.2±0.2	0.03
Bond lengths	2.1±0.4	2.4
Bond angles	17.4±2.6	17.6
Improper angles	2.1±0.4	2.2
van der Waals repulsion	4.1±1.8	2.2

The notation of the NMR structures is as follows: ⟨*Compstatin*⟩ is the ensemble comprising the final 21 simulated annealing structures; $\overline{Compstatin}$ is the mean structure obtained by averaging the coordinates of the individual simulated annealing structures; $(\overline{Compstatin})_r$ is the restrained regularized mean structure obtained by restrained regularization of the mean structure $\overline{Compstatin}$.

The cyclic peptide Compstatin forms a type I β-turn spanning residues Gln^5-Asp^6-Trp^7-Gly^8 (Fig. 10, left and center panels). The general criteria for the presence of a β-turn are: a $C^{\alpha}(1)$-$C^{\alpha}(4)$ distance < 7 Å and that the central residues are not helical (Chou and Fasman, J. Mol. Biol. 115: 135-175, 1977; Schulz and Schirmer, Principles of Protein Structure, Spriger Verlag, NY, 1979; Rose et al., Adv. Prot. Chem. 37: 1-109, 1985; Wilmot and Thornton, J. Mol. Biol. 203: 221-232, 1988). The presence of a C=O(1)-HN(4) hydrogen bond

is possible but not necessary for stabilization of the β-turn (Chou and Fasman, 1977 *supra*). More specifically, a type I β-turn is characterized by dihedral angles $(\phi_2, \psi_2) = (-60°, -90°)$ and $(\phi_3, \psi_3) = (-90°, 0°)$ (Venkatachalam, Biopolymers 6: 1425-1436, 1968; Richardson, Adv. Prot. Chem. 34: 167-339, 1981; Rose et al., 1985 *supra*; Wilmot and Thornton 1988 *supra*). Table 4 compares the characteristic dihedral angles and distances of the average structure of Compstatin with the classic type I β-turn.

Table 4. Criteria for the formation of a type I β-turn.[a]

	ϕ_2	ψ_2	ϕ_3	ψ_3	$C^\alpha(1)$-$C^\alpha(4)$	C=O(1)-N(4)
Classic Type I β-turn	-60°±30°	-30°±30°	-90°±30°	0°±30°	< 7 Å	2-5 Å
<*Compstatin*> Type I *β*-turn	-65°±13°	-26°±8°	-108°±12°	-14°±3°	4.7±0.2 Å	3.3±0.4 Å
Compstatin Type I β-turn	-76°	-23°	-100°	-14°	4.8 Å	3.4 Å

[a]The notation for the Compstatin structures is as in Table 2.
[b]The Compstatin β-turn spans the segment Gln^5-Asp^6-Trp^7-Gly^8.

Type I β-turns are the most abundant turns in protein and peptide structures, and they are two to three times more common than any of the other major categories, the type II or type III turns; the rest are very rare (Schulz and Schirmer, 1979 *supra*; Wilmot and Thornton, 1988 *supra*). Position 4 of the Compstatin β-turn is occupied by Gly, which has been found to be by far the most favorable amino acid in the fourth position of a type I turn (Wilmot and Thornton, 1988 *supra*). Likewise, position 2 of the β-turn of Compstatin is occupied by Asp, which has been found to be one of the most favorable amino acids in type I β-turns (Wilmot and Thornton, 1988 *supra*).

Figure 10, right panel, shows a space-filling model of the average restrained regularized structure of Compstatin. Long range spatial contacts between the rings of His^9 and Trp^7 with Gly^8, Gln^5 and Asp^6 are consistent with observed NOEs. A clustering of hydrophobic side chains of Val^3, Val^4 and Trp^7 was observed.

Figure 11, lower panel, shows the fractional solvent accessibility of each residue of Compstatin. Fractional solvent accessibility is defined as the percent value of the ratio of the solvent-accessible area (Lee & Richards, J. Mol. Biol. 55: 379-400, 1971) of each residue of the peptide over the total surface area of the isolated residue. The calculation was performed with the program MOLMOL (Koradi et al., J. Mol. Graphics 14: 51-55, 1996) using the average restrained regularized structure of Compstatin and a water molecule probe radius of 1.4 Å. Reduced solvent accessibility was observed for Gln^5 and Gly^8 at the two ends of the β-turn. This is probably the effect of capping of the turn by the rings of Trp^7 because of hydrophobic clustering towards the side chains of Val^3 and Val^4. Also, reduced surface accessibility was observed at Cys^2 and Cys^{12}, presumably due to restriction of the side chains by the disulfide bond.

Consistency of the calculated structures with the NMR parameters. There are several direct NMR criteria for the detection of β-turns, such as characteristic NOE connectivities, $^3J_{NH-H\alpha}$-coupling constants, temperature coefficients and chemical shifts (Wüthrich, 1986 *supra*; Dyson et al., J. Mol. Biol. 201: 161-200, 1988; Dyson and Wright, Ann. Rev. Biophys. Biophys. Chem. 20: 519-538, 1991; Dyson and Wright, 1995 *supra*). However, in several instances the presence of multiple peptide conformers can produce an averaging of the NMR parameters that can hinder a straightforward analysis (Dyson et al., 1988 *supra*). In these cases the NMR parameters, alone and in the absence of a complete structure calculation, might

not be sufficient to detect classical β-turns, but they should be consistent with the definition of a particular turn-type (Wüthrich, 1986 *supra*). The consistency of the measured NMR parameters with the calculated average structure of Compstatin is discussed below.

In general, the NOEs that are consistent with the presence of β-turns are NH(2)-NH(3), NH(3)-NH(4), H^{α}(2)-NH(3), H^{α}(3)-NH(4) and H^{α}(2)-NH(4) (Wüthrich, 1986 *supra*). In the case of an ideal Type I β-turn strong NH(2)-NH(3) (corresponding to a distance of 2.6 Å), NH(3)-NH(4) (2.4 Å), medium H^{α}(2)-NH(3) (3.4 Å), H^{α}(3)-NH(4) (3.2 Å) and weak H^{α}(2)-NH(4) (3.6 Å) NOEs are observed. NOEs that distinguish a Type I from a Type II β-turn are: a strong NH(2)-NH(3) NOE (2.6 Å) and a medium H^{α}(2)-NH(3) NOE (3.4 Å) in an ideal Type I β-turn, as opposed to a weak NH(2)-NH(3) NOE (4.5 Å) and a strong H^{α}(2)-NH(3) NOE (2.2 Å) in an ideal Type II turn. In the case of Compstatin a strong NH(3)-NH(4) (compared to other NH-NH) NOE was observed between Trp^{7} and Gly^{8}, a finding that is therefore consistent with the presence of a β-turn (Type I or II). A strong NH(2)-NH(3) NOE was observed between residues Asp^{6} and Trp^{7} indicating the presence of a Type I β-turn. The other characteristic of a Type I β-turn, a medium H^{α}(2)-NH(3) NOE between Asp^{6} and Trp^{7}, could not be unambiguously assigned because of overlap with the strong intra-residue Trp^{7} NH-H^{β} NOE (the H^{α} of Asp^{6} and Trp^{7} were at 4.56 and 4.57 ppm, respectively; Table 2). Increasing the temperature from 5°C to 10°C did not resolve this ambiguity because of the small effect of temperature on α-protons. Finally, for a similar reason the H^{α}(2)-NH(4) weak NOE between Asp^{6} and Gly^{8} could not be distinguished from the medium H^{α}(3)-NH(4) NOE between Trp^{7} and Gly^{8} (Table 2). More specifically, a medium NOE at (H^{α}, NH)=(4.57, 8.47) ppm was observed, which most likely corresponds to the medium expected H^{α}(3)-NH(4) NOE between Trp^{7} and Gly^{8}, (characteristic of a β-turn). This NOE

hinders the unambiguous assignment of the expected weak $H^{\alpha}(2)$-NH(4) NOE between Asp^{6} and Gly^{8} (also characteristic of a β-turn). This is due to the overlap of the H^{α}-resonances of Asp^{6} and Trp^{7} (Table 2). The temperature increase to 10°C did not resolve this ambiguity. However, an $H^{\beta}(2)$-NH(4) very weak NOE between Asp^{6} and Gly^{8} was observed in the 200 ms NOESY spectrum; this NOE gained significant intensity in the 400 ms NOESY spectrum, where some degree of spin diffusion is present.

In addition to NOEs, $^{3}J_{NH-H\alpha}$-coupling constants can be used to validate the presence of a β-turn (Wüthrich, 1986 *supra*). However, $^{3}J_{NH-H\alpha}$-coupling constants should only be used in a qualitative and relative way in NMR structural analysis of peptides (*vide supra*), not only because of the difficulty in measuring and interpreting $^{3}J_{NH-H\alpha}$-coupling constants from NMR data (*vide supra*) but also because of conformational averaging. Absence of any $^{3}J_{NH-H\alpha} < 6$ Hz (Fig. 9) suggests that Compstatin is quite flexible and possibly exists in a conformational equilibrium between helical and extended dihedral angle space. The $^{3}J_{NH-H\alpha}$-coupling constant values of $^{3}J_{NH-H\alpha}(2) \approx 4$ Hz and $^{3}J_{NH-H\alpha}(3) \approx 9$ Hz are consistent with the presence of a Type I β-turn and help to distinguish a Type I from a Type II β-turn (the latter having $^{3}J_{NH-H\alpha}(3) \approx 5$ Hz) (Wüthrich, 1986 *supra*). In the case of Compstatin a small $^{3}J_{NH-H\alpha}(2)$-coupling constant for Asp^{6} relative to a large $^{3}J_{NH-H\alpha}(3)$-coupling constant for Trp^{7} was observed (Fig. 9), another finding that is consistent with the presence of a Type I β-turn.

$^{3}J_{NH-H\alpha}$-coupling constants have been used to evaluate the population of the β-turn conformer in peptides, on the basis of the $^{3}J_{NH-H\alpha}$-value of residue 2 of the β-turn (Campbell et al., Biochemistry 34: 16255-16268, 1995). The averaging of $^{3}J_{NH-H\alpha}(2)$ reflects the presence of an equilibrium between different structural conformers. Assuming a 2-state model of a β-turn and an

extended conformation, a 100% β-turn conformer corresponds to $^3J_{NH-H\alpha}(2)=4$ Hz (or $\phi_2=-60°$) and a 100% extended conformer corresponds to $^3J_{NH-H\alpha}(2)=9$ Hz (or $\phi_2<-100°$). Using this model and a $^3J_{NH-H\alpha}(2)=6.9$ Hz for Asp^6 at position 2 of the β-turn ($^3J_{NH-H\alpha}$ extracted with the Kim and Prestegard method, 1989 *supra*, Fig. 2), we calculated a β-turn conformation of 42%. Accounting for an estimated error of 1 Hz in measuring $^3J_{NH-H\alpha}$-coupling constants and the fact that the $^3J_{NH-H\alpha}$-coupling constants extracted from DQF-COSY spectra might represent an upper limit of the actual $^3J_{NH-H\alpha}$-value, we estimate that a β-turn population of 42% to 63% is present in the case of Compstatin.

Deviations of observed chemical shifts from random coil values are indicative of the presence of secondary structure. For α-protons, a mean difference of -0.39 ppm or of +0.37 ppm is indicative of a helical or an extended conformation, respectively (Wishart et al., J. Mol. Biol. 222: 311-333, 1991). Figure 12, upper panel, shows the difference in observed minus random coil values (Merutka et al., 1995 *supra*) for the α-protons of Compstatin at 5°C. No α-proton chemical shift difference greater than ±0.3 ppm was observed. Thus it appears that there is no strong preference for a helical or extended conformation and that Compstatin is found in a rather flexible conformational environment.

Figure 12, lower panel, shows the temperature dependence of the amide protons of Compstatin. The region between the two solid lines corresponds to the temperature dependence of amino acids in random coil GGXGG peptides with temperature coefficients in the range $6 \leq -(\Delta\delta/\Delta T)\times 1000 \leq 10$ ppb/K (Merutka et al., 1995 *supra*). It has been suggested that amide protons that are protected from exchange with solvent and possibly hydrogen bonded have temperature coefficients $-(\Delta\delta/\Delta T)\times 1000 \leq 5$ ppb/K (Rose et al., 1985 *supra*). This translates to $\Delta\delta \geq -0.025$ ppm (values higher than the dotted line in Fig. 12, lower

panel). An error of 0.01 ppm in the measurement of chemical shifts should also be taken into account (Table 2). On the basis of the chemical shift data in Figure 12, lower panel, the NH of Gly^8 does not appear to be hydrogen-bonded. This situation is not unusual, as hydrogen bonding is not necessary for β-turn stabilization (Chou and Fasman, 1977 *supra*). However, the structure calculations place the NH of Gly^8 in the proximity of the carbonyl group of Gln^5 as the C=O(1)-N(4) distance has been found to be 3.3±0.4 Å in the ensemble of the family of the 21 calculated structures (Table 3). Various authors report the hydrogen-bonding distance between the C=O(1) and N(4) as 3.4±0.1 Å (Chou and Fasman, 1977 *supra*; Rose et al., 1985 *supra*; Wilmot and Thornton, 1988 *supra*). In the case of Compstatin the C=O(1)-N(4) distance appears to be at the borderline of the definition of a hydrogen bond, according to the structure calculation. The opposite effect of temperature on the amide chemical shift of Trp^7 and on the rest of the residues is probably a result of the aromatic effect of the Trp^7 rings (Kemmink et al., J. Mol. Biol. 230: 312-322, 1993).

Biological significance and structural determinants important in Compstatin-C3 binding.

Complement-mediated pathology has been reported in several diseases; thus, a specific complement inhibitor of therapeutic value needs to be developed. However, none is currently available. It is well known that activation of one pathway (classical or alternative, or lectin) leads to recruitment of other. For example, activation of the classical pathway results in the activation of the alternative pathway. Similarly, activation of the lectin pathway supports the activation of the alternative pathway. Thus, in most clinical conditions multiple pathways are activated. These results suggest the usefulness of a complement inhibitor that blocks all three pathways. The three pathways

converge at the C3 activation step; therefore, blocking this step would result in total shutoff of the complement cascade including generation of C3a and C5a and MAC formation. In fact, many physiological regulators of complement, e.g. factor H, CR1, DAF and MCP, act on C3b to inhibit complement activation. A soluble form of CR1 has been tested and found to suppress complement pathology in a number of *in vivo* complement-dependent diseases models (Kalli et al. 1994 *supra*). However identifying a smaller biologically active fragment of these regulatory proteins or a peptide mimetic is necessary for structural studies and the rational design of a clinical drug.

As described in Example 1, in order to identify the residues essential for Compstatin interaction with C3, we have synthesized a 11-residue peptide that has the sequence of Compstatin, except for Ile^{1} and Thr^{13}, and also generated nine Ala mutants in which each amino acid between Cys^{2} and Cys^{12} was replaced (we followed the notation of Compstatin after sequence alignment). Replacement of Val^{4}, His^{10} and Arg^{11} resulted in minimal change in the functional activity, suggesting that these residues do not contribute significantly to binding with C3 (see Table 1). Replacement of Val^{3}, Gln^{5}, Asp^{6} and Trp^{7} reduced the activity of the peptide by 6- to 36-fold. Replacing Gly^{8} dramatically reduced the activity of the peptide by more than 100-fold. It is interesting that four of these five residues comprise the Type I β-turn of Compstatin. The calculated Type I β-turn segment (Gln^{5}-Asp^{6}-Trp^{7}-Gly^{8}) is therefore most likely part of the binding site for C3. The total loss of biological activity that resulted from replacement of Gly^{8} is probably related to loss of the turn structure. Given the amino acid composition of the turn, Gly^{8} might be needed to release the steric hindrance and stabilize the turn structure. Of the four residues that comprise the Type I β-turn it seems that the two end-residues, Gln^{5} and Gly^{8}, which are somehow buried (as demonstrated by the

solvent accessibility calculation *vide supra*, Fig. 11, lower panel), are more essential for Compstatin activity (Table 2). However, the role of Val^3 in peptide binding is not obvious. As discussed above, a hydrophobic clustering of the side chains of Val^3, Val^4 and Trp^7 is present in Compstatin. Some interaction between the side chains of Val^3 and Asp^6 is observed in the calculated structure, which might assist in stabilizing the β-turn.

Peptide conformational changes upon binding have been observed by NMR spectroscopy, with a most common case that of the cyclophilin-cyclosporine complex (Weber et al., Biochemistry 30: 6563-6574, 1991; Wüthrich et al., 1991 *supra*). In the case of cyclosporine complexed to cyclophilin, inversion of the orientation of the dominant hydrophobic cluster and the peptide backbone, together with the presence of intermolecular hydrogen bonding, have been shown to be important for recognition and binding (Weber et al., 1991 *supra*; Wüthrich et al., 1991 *supra*). Likewise, it has recently been suggested that during the regulation of apoptosis the Bcl-x_L receptor protein undergoes structural reorientation to expose a hydrophobic segment upon binding of the Bak peptide (Sattler et al., Science 275: 983-986, 1997). The hydrophobic cluster of Compstatin might be mediating hydrophobic interactions with C3 through its binding site. The presence of a negative charge in Asp^6 at the second position of the β-turn and the possible role of this residue in charge-charge interactions during binding, together with hydrogen-bonding possibilities involving the side chains of Gln^5 and Asp^6, may be important for binding and biological activity.

The present invention is not limited to the embodiments specifically described and exemplified above, but is capable of variation and modification within the scope of the appended claims.

What is claimed is:

1. A compound that inhibits complement activation, which comprises a structural analog of residues 5 through 8 of a disulfide bridged form of Sequence I.D. No. 2, said compound having a constrained backbone conformation comprising a β-turn.

2. The compound of claim 1, wherein the β-turn is a Type I β-turn.

3. The compound of claim 1, which further comprises:

a) an N-terminal extension comprising a tripeptide or tetrapeptide, or mimetic thereof, of flexible backbone conformation;

b) a C-terminal extension comprising a tetrapeptide or pentapeptide, or mimetic thereof, of flexible backbone conformation.

4. The compound of claim 3, wherein the N-terminal extension comprises a structural analog of residues 1 or 2 through 4 of Sequence I.D. No. 2 and the C-terminal extension comprises a structural analog of residues 9 through 12 or 13 of Sequence I.D. No. 2.

5. The compound of claim 4, wherein the analog of residue 2 of Sequence I.D. No. 2 forms a bond with the analog of residue 12 of Sequence I.D. No. 2, of length and angle equivalent to a disulfide bond.

6. The compound of claim 4, wherein the analogs of residues 3 and 7 of Sequence I.D. No. 2 comprise hydrophobic side chains.

7. An oligopeptide or peptidomimetic structural analog of a disulfide bridged form of Sequence I.D. No. 2, comprising:

a) an N-terminal segment of flexible backbone conformation, corresponding to residues 1 or 2 through 4 of Sequence I.D. No. 2;

b) a central segment having a backbone conformation comprising a Type I β-turn, corresponding to residues 5 through 8 of Sequence I.D. No. 2; and

c) a C-terminal segment of flexible backbone conformation, corresponding to residues 9 through 12 or 13 of Sequence I.D. No. 2.

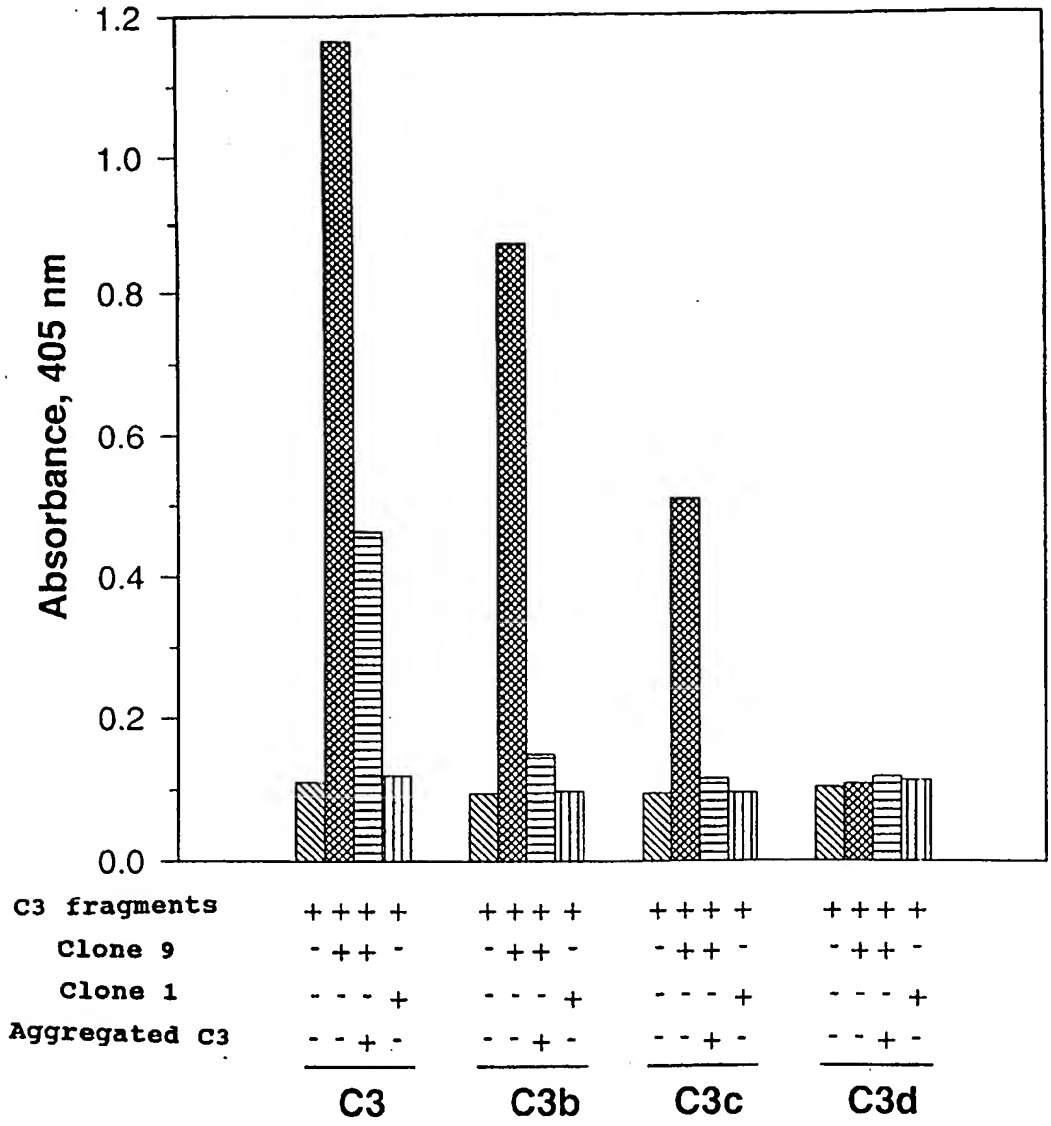
1.2
1.0
0.8
0.6
0.4
0.2
0.0
Absorbance, 405 nm
C3 fragments + + + + + + + + + + + + + + + +
Clone 9 - + + - - + + - - + + - - + + -
Clone 1 - - - + - - - + - - - + - - - +
Aggregated C3 - - + - - - + - - - + - - - + -
C3
C3b
C3c
C3d

FIGURE 1

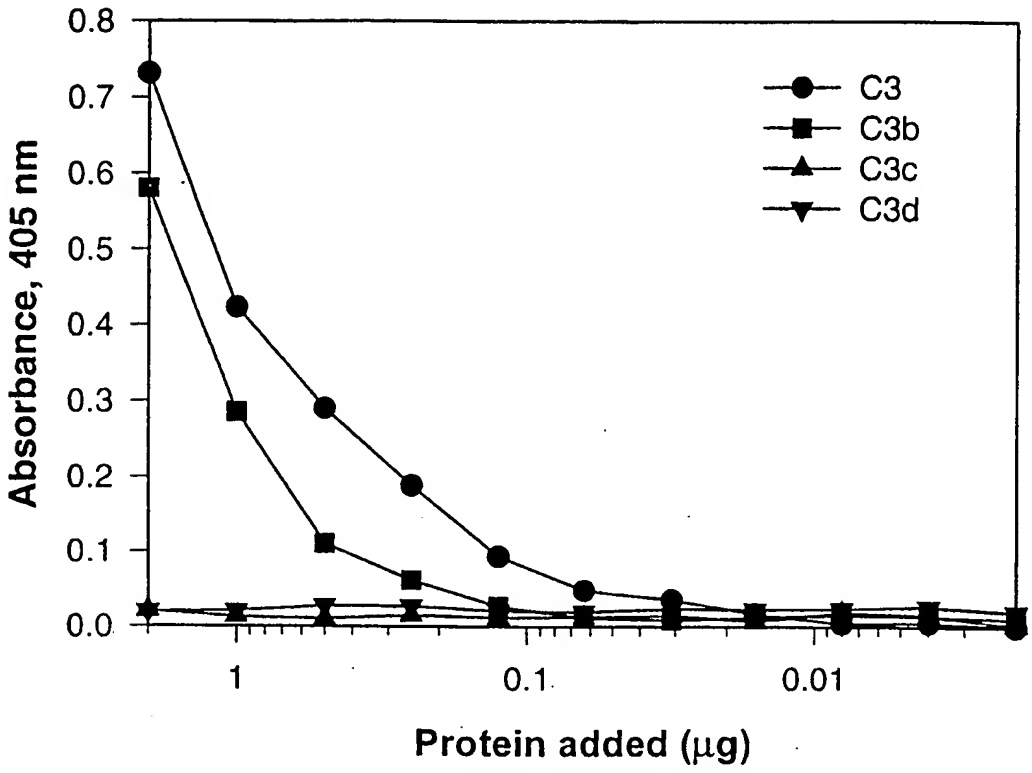
0.8
0.7
0.6
0.5
0.4
0.3
0.2
0.1
0.0
Absorbance, 405 nm
C3
C3b
C3c
C3d
1
0.1
0.01
Protein added (μg)

FIGURE 2

FIGURE 3A 3/12

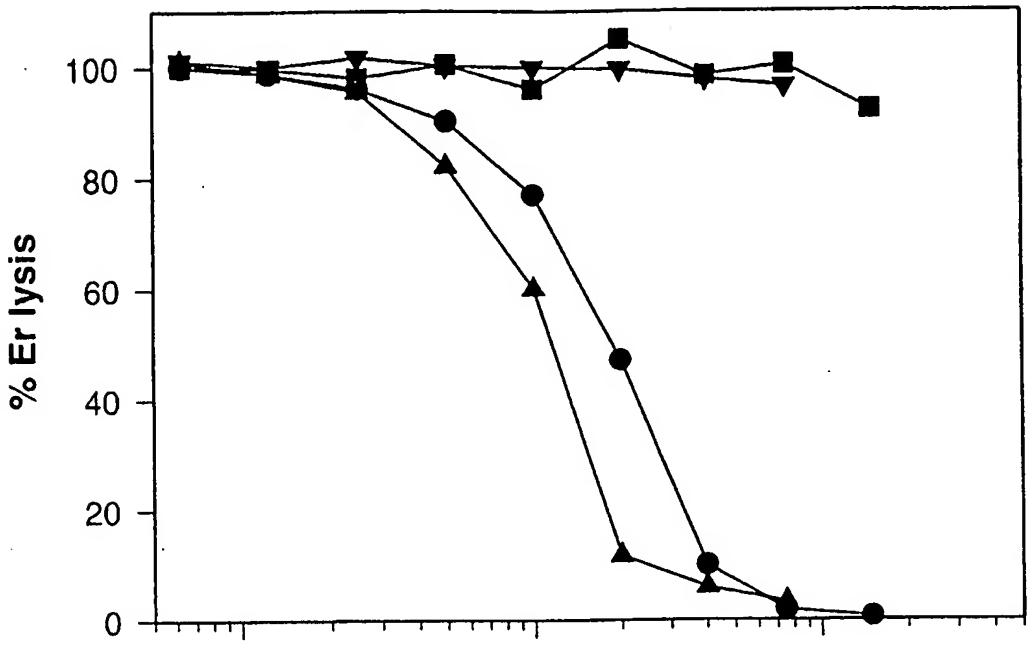

FIGURE 3B

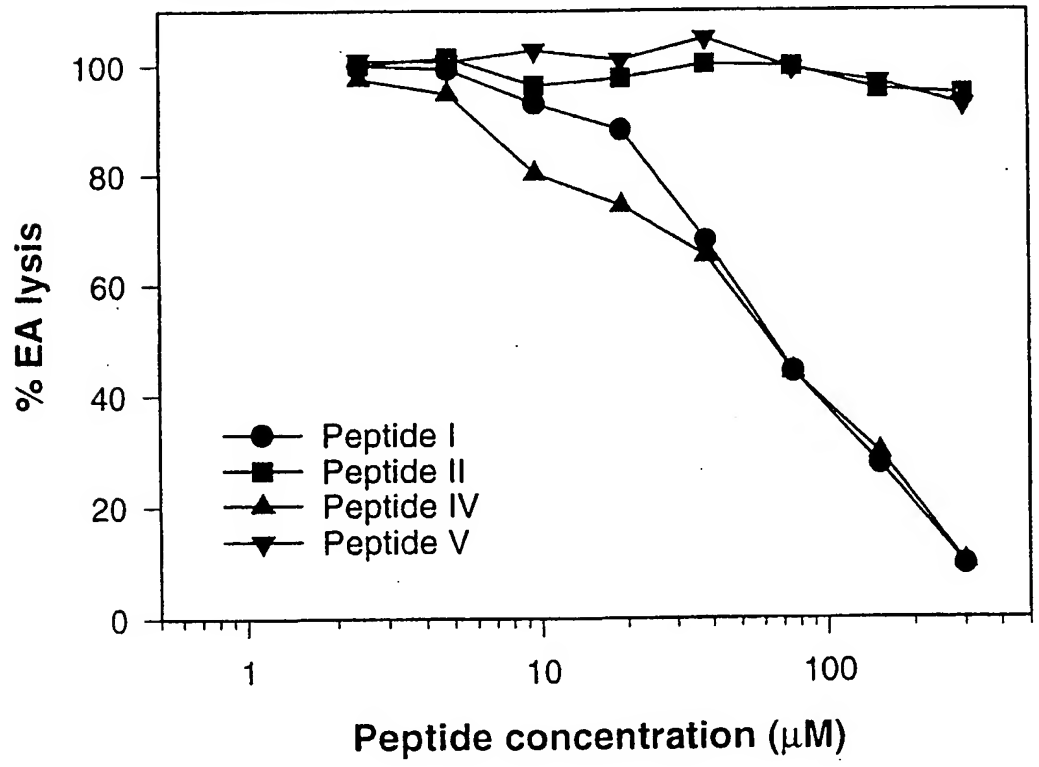

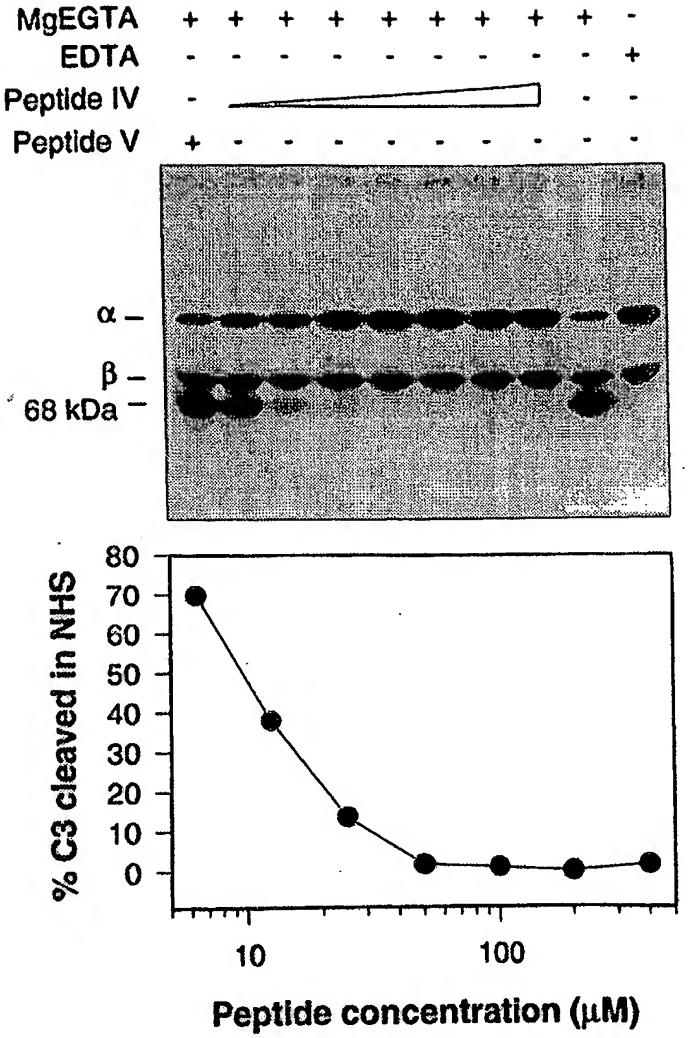
MgEGTA + + + + + + + + + -
EDTA - - - - - - - - - +
Peptide IV - - -
Peptide V + - - - - - - - - -
α –
β –
68 kDa –
% C3 cleaved in NHS
80
70
60
50
40
30
20
10
0
10
100
Peptide concentration (μM)

FIG. 4

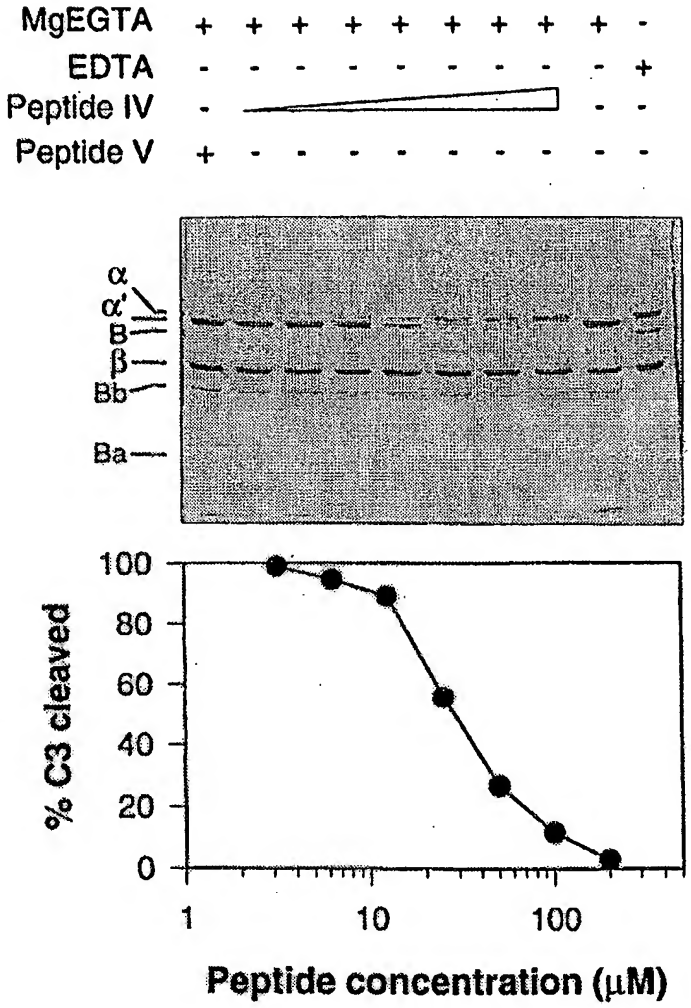
MgEGTA + + + + + + + + + -
EDTA - - - - - - - - - +
Peptide IV - - -
Peptide V + - - - - - - - - -
α
α'
B
β
Bb
Ba
100
80
60
40
20
0
% C3 cleaved
1
10
100
Peptide concentration (μM)

FIG. 5

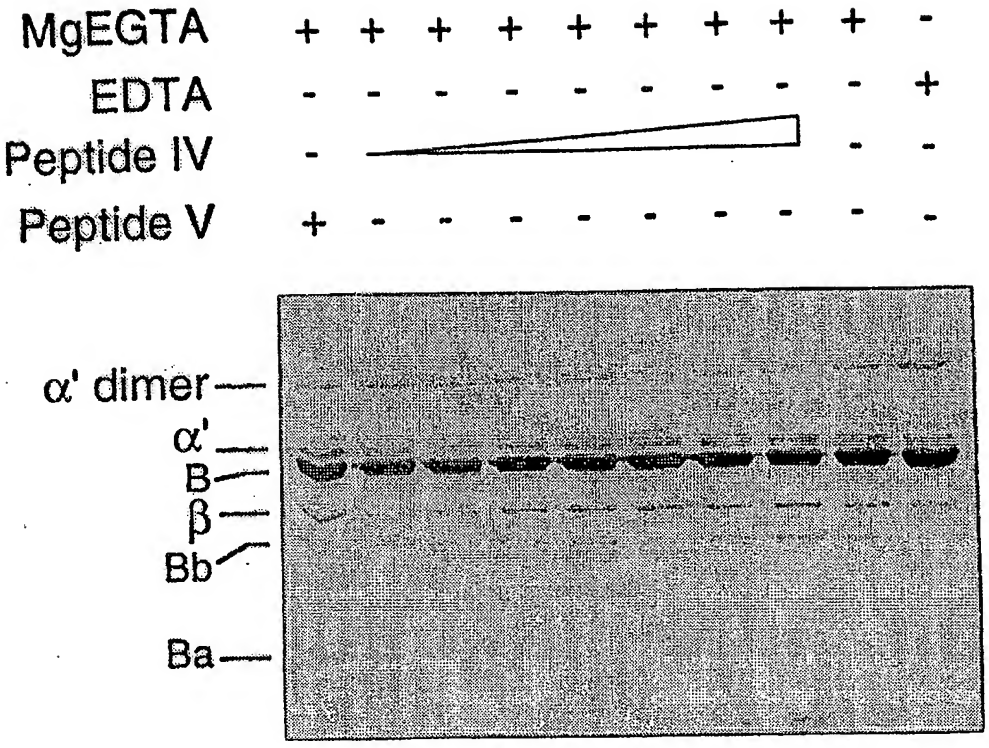

FIG. 6

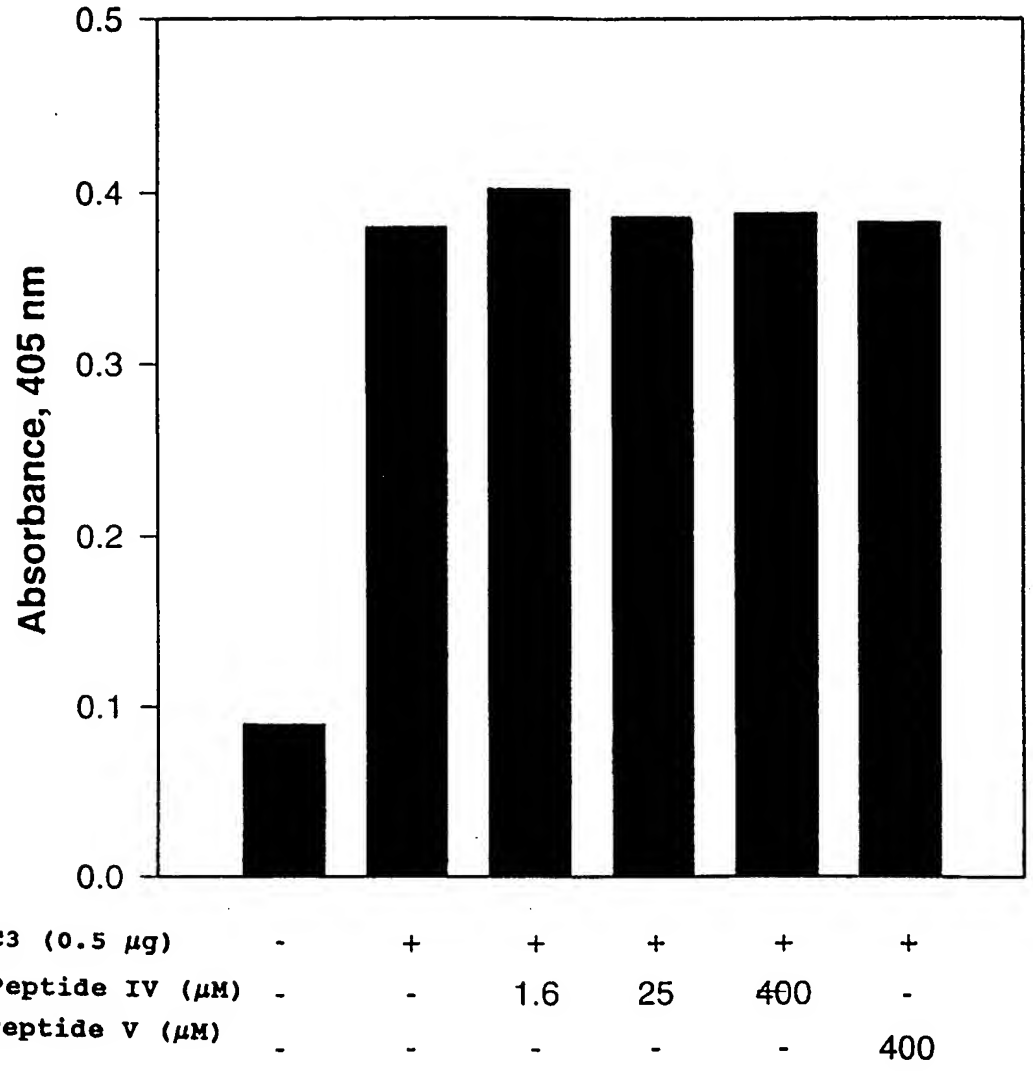
0.5
0.4
0.3
0.2
0.1
0.0
Absorbance, 405 nm
C3 (0.5 µg) - + + + + +
Peptide IV (µM) - - 1.6 25 400 -
Peptide V (µM) - - - - - 400

FIGURE 7

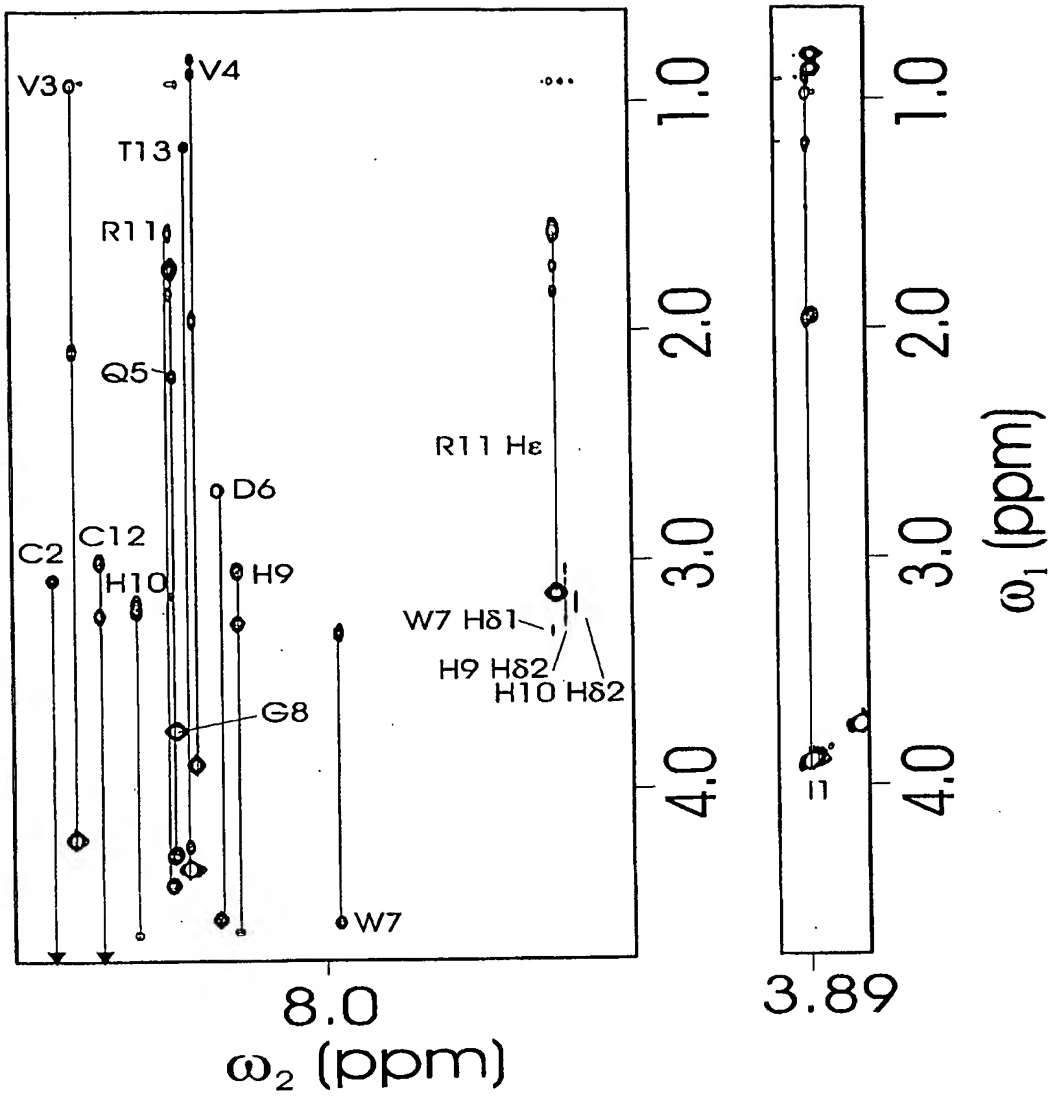
V3
V4
T13
R11
Q5
D6
C12
C2
H10
H9
G8
W7
R11 Hε
W7 Hδ1
H9 Hδ2
H10 Hδ2
1.0
2.0
3.0
4.0
8.0
ω2 (ppm)
3.89
ω1 (ppm)

FIGURE 8

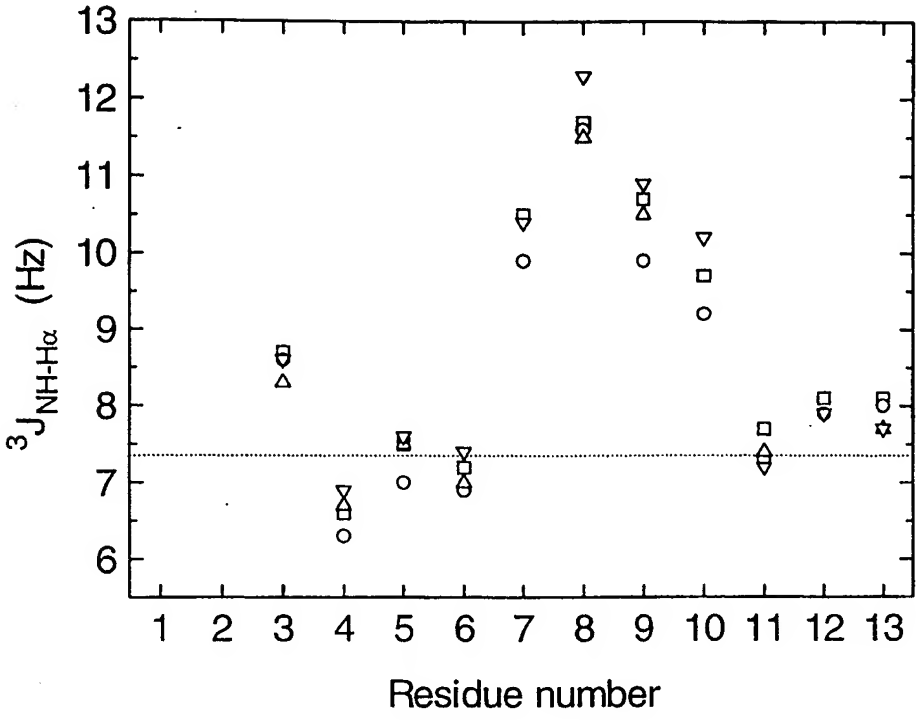
13
12
11
10
9
8
7
6
$^3J_{NH-H\alpha}$ (Hz)
1 2 3 4 5 6 7 8 9 10 11 12 13
Residue number

FIGURE 9

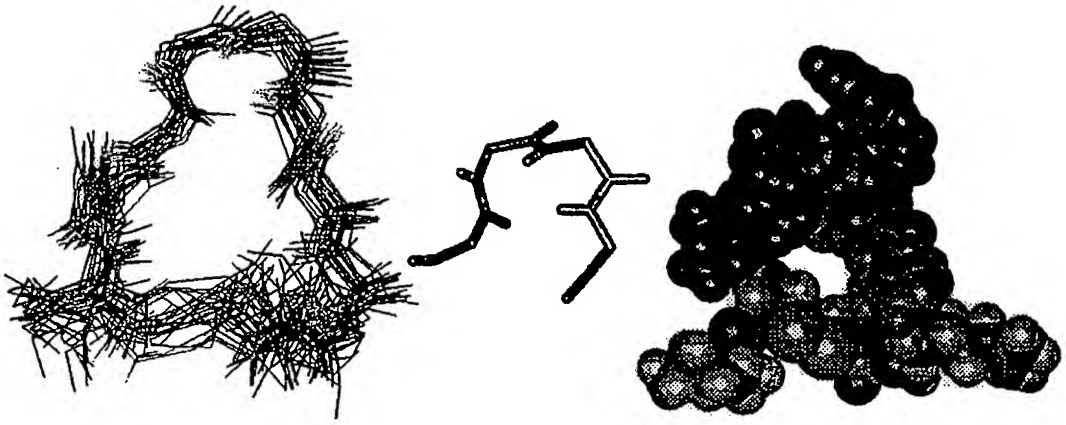

FIGURE 10

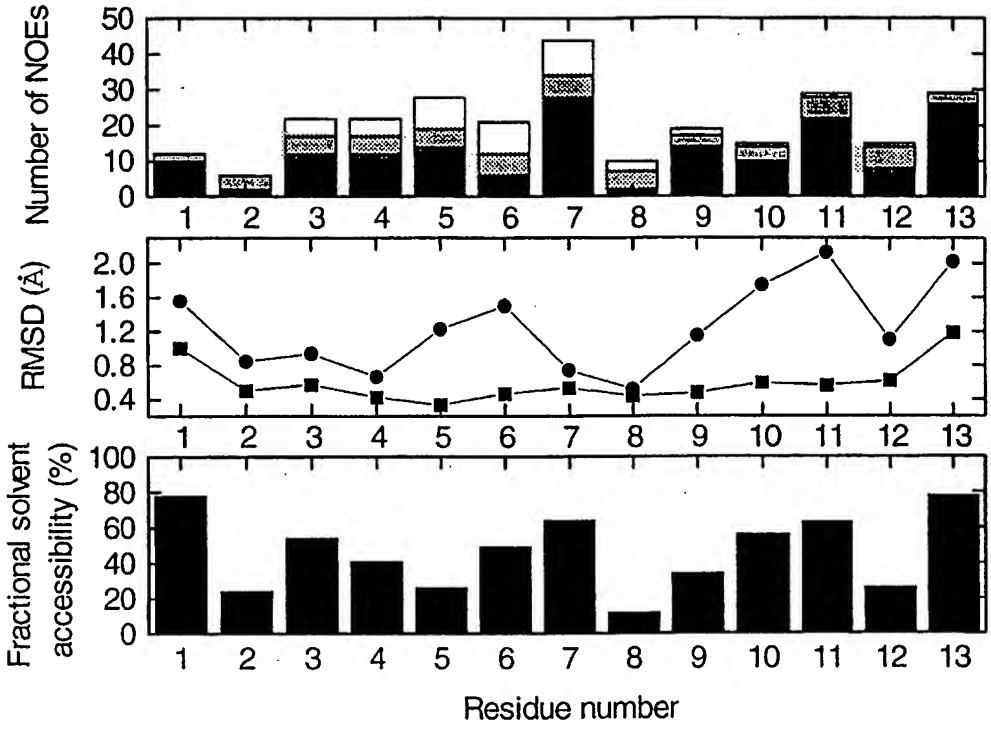
Number of NOEs
50
40
30
20
10
0
1 2 3 4 5 6 7 8 9 10 11 12 13
RMSD (Å)
2.0
1.6
1.2
0.8
0.4
1 2 3 4 5 6 7 8 9 10 11 12 13
Fractional solvent accessibility (%)
100
80
60
40
20
0
1 2 3 4 5 6 7 8 9 10 11 12 13
Residue number

FIGURE 11

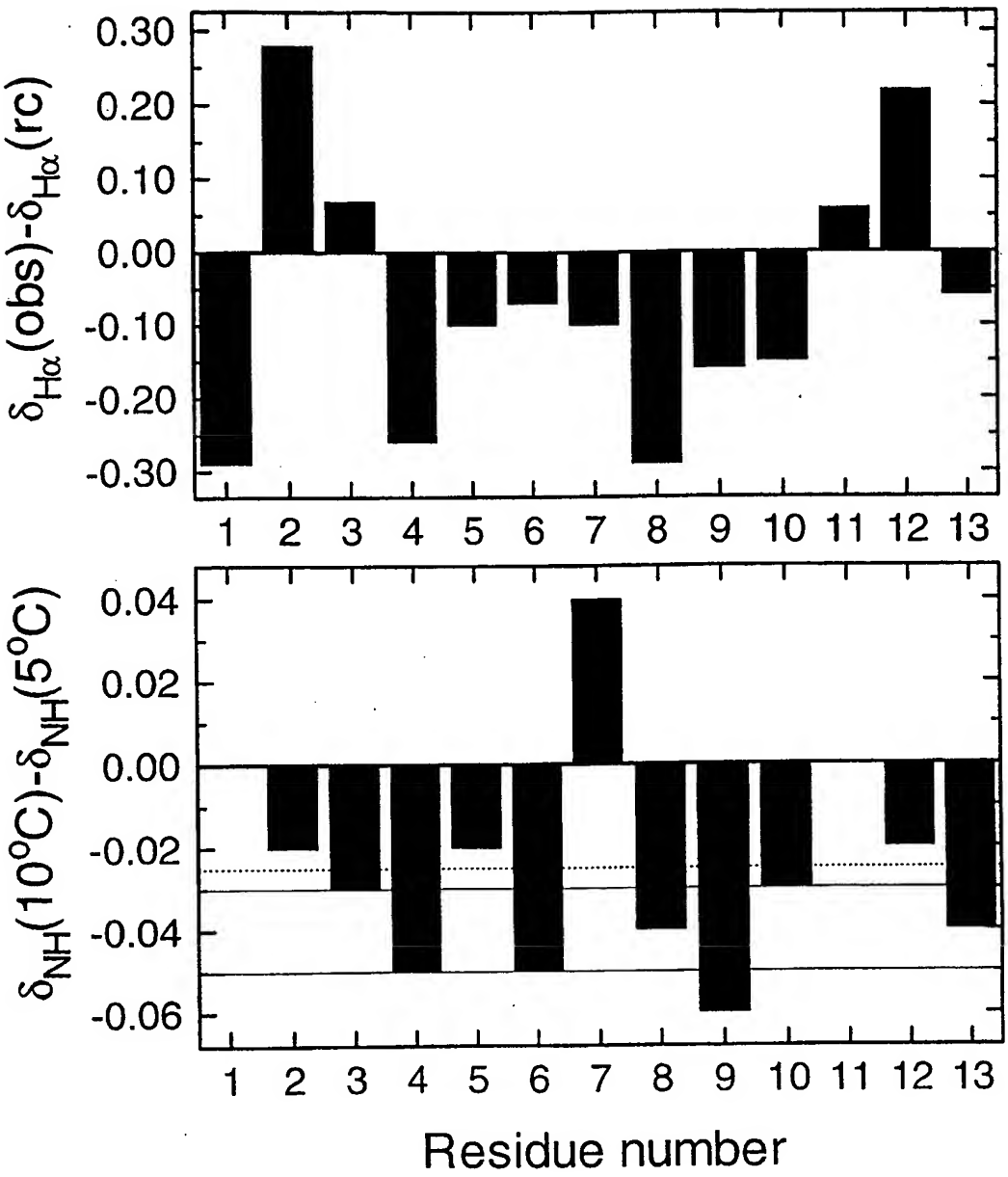
0.30
0.20
0.10
0.00
-0.10
-0.20
-0.30
$\delta_{H\alpha}$(obs)-$\delta_{H\alpha}$(rc)
1 2 3 4 5 6 7 8 9 10 11 12 13
0.04
0.02
0.00
-0.02
-0.04
-0.06
δ_{NH}(10°C)-δ_{NH}(5°C)
1 2 3 4 5 6 7 8 9 10 11 12 13
Residue number

FIGURE 12

INTERNATIONAL SEARCH REPORT

International application No.
PCT/US97/16850

A. CLASSIFICATION OF SUBJECT MATTER
IPC(6) :A 61K 38/10
US CL :514/14
According to International Patent Classification (IPC) or to both national classification and IPC

B. FIELDS SEARCHED

Minimum documentation searched (classification system followed by classification symbols)
U.S. : 514/14

Documentation searched other than minimum documentation to the extent that such documents are included in the fields searched
NONE

Electronic data base consulted during the international search (name of data base and, where practicable, search terms used)
APS, MEDLINE, EMBASE, SCISEARCH, DERWENT WORLD PATENT, REGISTRY, GENESEQ28, SWISS-PROT34

C. DOCUMENTS CONSIDERED TO BE RELEVANT

Category*	Citation of document, with indication, where appropriate, of the relevant passages	Relevant to claim No.
Y	BECHERER et al. Identification Of The C3b Receptor-Binding Domain In Third Component Of Complement. Journal of Biol. Chem. 05 October 1988. Vol. 263. No. 28. pages 14608-14591, see entire article.	1-7
Y	SAHU et al. Inhibition Of Human Complement By A C3-Binding Peptide Isolated From A Phage-Displayed Random Peptide Library. 1996. Journal of of Immunology. Vol. 157. pages 884-891, see entire article.	1-7
Y	LAMBRIS et al. A Discontinuous Factor H Binding Site In The Third Component of Complement As Delineated By Synthetic Peptides. Journal of Biological Chemistry. 25 August 1988. Vol. 263. No. 24. pages 12147-12150, see entire article.	1-7

☐ Further documents are listed in the continuation of Box C. ☐ See patent family annex.

*	Special categories of cited documents:	"T"	later document published after the international filing date or priority date and not in conflict with the application but cited to understand the principle or theory underlying the invention
"A"	document defining the general state of the art which is not considered to be of particular relevance	"X"	document of particular relevance; the claimed invention cannot be considered novel or cannot be considered to involve an inventive step when the document is taken alone
"E"	earlier document published on or after the international filing date	"Y"	document of particular relevance; the claimed invention cannot be considered to involve an inventive step when the document is combined with one or more other such documents, such combination being obvious to a person skilled in the art
"L"	document which may throw doubts on priority claim(s) or which is cited to establish the publication date of another citation or other special reason (as specified)	"&"	document member of the same patent family
"O"	document referring to an oral disclosure, use, exhibition or other means		
"P"	document published prior to the international filing date but later than the priority date claimed		

Date of the actual completion of the international search 28 NOVEMBER 1997	Date of mailing of the international search report 14 JAN 1998
Name and mailing address of the ISA/US Commissioner of Patents and Trademarks Box PCT Washington, D.C. 20231 Facsimile No. (703) 305-3230	Authorized officer MARTHA LUBET Telephone No. (703) 308-0196

Form PCT/ISA/210 (second sheet)(July 1992)*